39

WET GRANULATION PROCESSES

KAREN P. HAPGOOD
Department of Chemical Engineering, Monash University, Clayton, VIC, Australia

JAMES D. LITSTER
School of Chemical Engineering and Department of Industrial & Physical Pharmacy, Purdue University, West Layafette, IN, USA

39.1 INTRODUCTION

Granulation is a size enlargement process, where individual powder particles, usually of several different components, are aggregated together to form a larger structured particle where the original particles can still be distinguished. Granulation of one or more drugs and excipients is a common first step in the manufacture of tablets or capsules for pharmaceutical drug delivery. Although direct compression is possible, granulation usually ensures good flow properties and uniform bulk density essential for tabletting, and reduces the risk of segregation by creating multicomponent granules with more uniform composition than the dry blend. Dry granulation, also known as roller compaction, uses compressive forces to form the aggregates, and is covered in detail in Chapter 38.

In this chapter, we focus on wet granulation, where a liquid is used to form wet agglomerates, which are subsequently dried. We first provide an overview of the many advances in our understanding of the science underlying wet granulation. In the second half of the chapter, we discuss scale-up approaches and provide a case study of how the mechanistic knowledge can be applied to design the granulation process and scale-up with minimal trial-and-error. We conclude with some future directions for granulation process development and manufacturing in the pharmaceutical industry.

39.2 MECHANISMS IN WET GRANULATION

Wet granulation is the process of using liquid and a binder material (usually a polymer such as HPC, PVP, HMPC) to aggregate the individual particles in the dry mix into particle assemblies. The assemblies contain a mixture of drug and excipients, and have a porous structure, which provides improved compression properties due to the rearrangement of particles during the collapse of the granule structure. There are three main stages in granulation [1] (refer to Figure 39.1), which are as follows:

1. *Nucleation and Wetting*: In this stage, the spray drops form the initial granules or nuclei.
2. *Consolidation and Growth*: Agitation leads to granule–granule collisions and granule–particle collisions, resulting in larger granules—this is a size enlargement process. These collisions may also result in a reduction in internal pore space of the granule—this densification process is termed as consolidation.
3. *Attrition and Breakage*: Agitation forces exceeding granule strength will result in either fracture of the granule into several large pieces, or attrition of the outer layer of particles from the granule. These are both size reduction processes, and both may occur simultaneously.

Chemical Engineering in the Pharmaceutical Industry: R&D to Manufacturing Edited by David J. am Ende

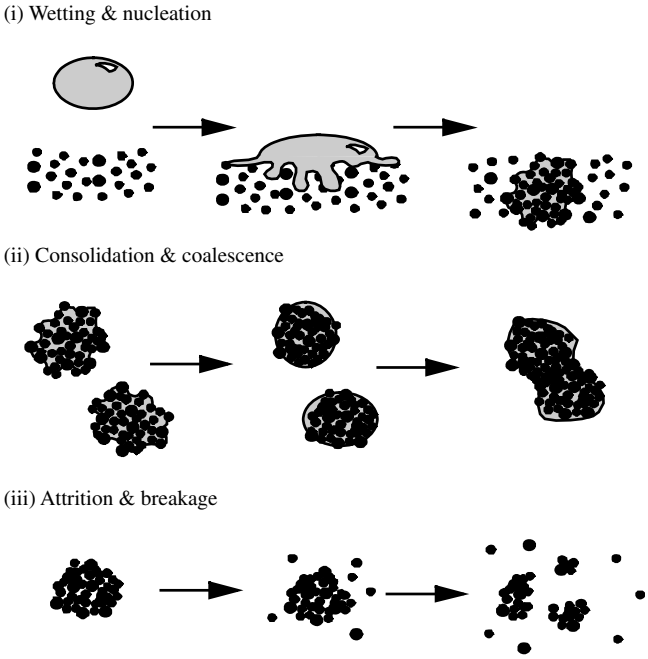

FIGURE 39.1 Rate processes in granulation (i) wetting and nucleation; (ii) consolidation and (iii) growth; and attrition and breakage [1].

Each mechanism is discussed in more detail below.

39.2.1 Nucleation

Mixing and distribution of the liquid during the nucleation phase (spraying phase) is an important step, and poor initial liquid distribution leads to a heterogeneous nuclei size distribution and increased variability in the granulation process [2]. Nuclei formed from under conditions of poor liquid distribution will have broad distributions of size, porosity, and saturations [2]. This in turn will lead to different growth and breakage rates for each granule. Ensuring a controlled nucleation step is the first step toward a controlled granulation process.

Immersion nucleation is the step where fine powders are engulfed by larger drops to form nuclei [3–5]. There are five steps in immersion nucleation as shown in Figure 39.2. Initially, the drop must be formed at the nozzle. After landing on the powder surface, the drop may potentially shatter and break into fragments, as shown experimentally [6] or

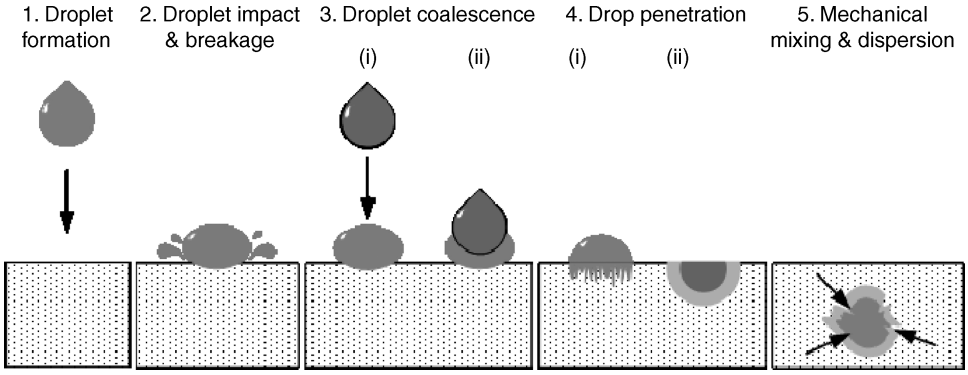

FIGURE 39.2 Five possible steps in immersion nucleation [10, 14]. (1) Droplet formation; (2) droplet impact and possible breakage on the powder bed; (3) droplet coalescence upon contact with other droplets at high spray flux; (4) drop penetration into the powder bed (i) and formation of a nucleus granule (ii); (5) mechanical mixing and dispersion of the liquid and powder.

coalesce with another drop already at the surface of the powder. Once it reaches the powder surface, the drop may penetrate into the powder bed via capillary action (step 4 in Figure 39.2), or it may require mechanical agitation and shear to disperse the fluid through the powder. A similar diagram for drops landing on a fluidized powder bed has also been published [7], which also depicts the nuclei passing through the spray zone multiple times. Distribution nucleation [3–5] can occur in fluid beds operated with very fine drops, which are of the same size or smaller than the particle size. The mechanisms of distribution nucleation are less well understood.

There are two parameters describing the immersion nucleation process in the spray zone of the granulator—the drop penetration time and the dimensionless spray flux [8, 9]. These parameters have been combined to form a nucleation regime map [10] and can be used for scale-up [11] and to quantitatively model the nuclei size distribution in the spray zone [12, 13].

39.2.1.1 Drop Penetration Time As the powder moves beneath the spray zone, the small droplets will land on the powder surface and begin to mix with the powder (see Figure 39.2). When the powder is easily wetted or hydrophilic, that is, the contact angle between the powder and fluid is less than 90°, penetration of the fluid into the powder pores will begin to occur. The rate at which a single drop of fluid, with volume V_d, viscosity μ, and surface tension γ_{lv} will penetrate into a static porous medium with cylindrical pores of radius R_{pore} and an overall porosity of ε is given by the drop penetration time t_p [15, 16]

$$t_p = 1.35 \frac{V_d^{2/3}}{\varepsilon^2 R_{pore}} \frac{\mu}{\gamma_{lv} \cos\theta} \tag{39.1}$$

In a loosely packed powder, similar to that found during agitation of the powder in the granulator, the voidage and pore size will be fairly heterogeneous. The powder will contain some combination of small pores and much larger pore spaces, or macrovoids. Liquid will flow through the small micropores, but there is no capillary driving force for the liquid to flow into the large macrovoids, as the rapid expansion of the pore radius dramatically reduces the Laplace pressure, which is the driving force for capillary flow. This means that the liquid does not flow through the macrovoids and must instead find a path around the macrovoid, slowing down the penetration [8] (Figure 39.3).

The effective voidage ε_{eff} is the first simple step toward including the effect of nonuniform pore structure on the penetration of a fluid into a real powder bed [8]. At the tap density ε_{tap}, the bed is assumed to contain no macrovoids. As the bed becomes less densely packed, the porosity of the bed increases, and the fraction of the voidage above the initial tapped bed voidage is assumed to form macrovoids.

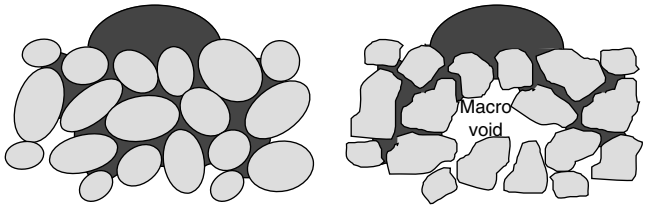

FIGURE 39.3 Liquid will penetrate the micropores which are driven by capillary action, but wherever a pore rapidly expands into a macrovoid, the fluid has to find a path around the flow obstruction [8].

The effective bed voidage thus estimates the amount of pore space that is actually available for capillary driven flow

$$\varepsilon_{eff} = \varepsilon_{tap}(1-\varepsilon+\varepsilon_{tap}) \tag{39.2}$$

The effective porosity is used in the Kozeny equation in place of overall bed porosity ε to estimate the effective micropore size R_{eff}, which is pore size available for liquid flow

$$R_{eff} = \frac{\varphi d_{32}}{3} \frac{\varepsilon_{eff}}{1-\varepsilon_{eff}} \tag{39.3}$$

Thus, the most appropriate equation for estimating the drop penetration time t_p into a loosely packed porous powder bed is [8]

$$t_p = 1.35 \frac{V_d^{2/3}}{\varepsilon_{eff}{}^2 R_{eff}} \frac{\mu}{\gamma_{lv} \cos\theta} \tag{39.4}$$

The drop penetration time is an indication of the kinetics of nucleus formation. Equation 39.4 shows that the penetration time depends on several factors, including the drop size V_d, the fluid properties (viscosity μ, surface tension γ_{lv}, and contact angle θ), and the powder packing structure (ε_{eff} and R_{eff}). However, the fluid viscosity has the largest effect, as the fluid viscosity can range over several orders of magnitude. This is also commonly found in pharmaceutical granulation, where low-viscosity fluids such as water or ethanol are used as frequently as high-viscosity fluids (e.g., a 7% HPC solution has a viscosity of 104 mPa s [9]). Figure 39.4 shows a water drop penetrating into a lactose powder bed over 2.3 s. In contrast, a similar drop of 7% HPC takes approximately 2 min to penetrate into the powder bed [8]. This timescale is clearly much longer than the timescale of agitation, and implies that nucleation via wetting and capillary action (step 4 in Figure 39.2) is not the dominant mechanism for high-viscosity systems. Instead, dispersion of the fluid through the powder will need to occur via mechanical mixing of the powder (see step 5 in Figure 39.2).

For a given powder, the drop penetration time is proportional to the liquid properties group $\mu/\gamma_{lv}\cos\theta$. For a given fluid, as the powder becomes finer (i.e., the d_{32} particle size decreases) the drop penetration time increases, primarily due

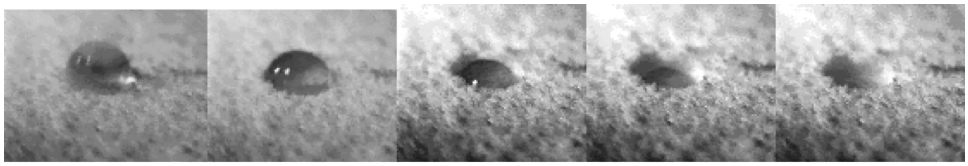

FIGURE 39.4 Water drop (~6 μL volume) penetrating into lactose powder. (a) Impact; (b) 0.23 s; (c) 0.9 s; (d) 1.4 s; and (e) 2.3 s (adapted from Ref. 8).

to a decrease in packing efficiency which creates a higher proportion of macrovoids [8]. Equation 39.4 can be used to estimate the drop penetration time from theory, but can have large errors for very fine, cohesive powders [8]. Experimental tests are recommended in this case, with equation 39.4 used to scale the experimental results to account for differences in drop size, etc. between the experiment and the actual manufacturing process (e.g., see Ref. 17).

Drop penetration time tends to decrease if the powder is already partially wet [14, 18], and the effect is more pronounced for viscous fluids with long penetration times [14]. For drops with long penetration times that land adjacent to a prewet patch of powder, the drop will tend to migrate over and penetrate into the preexisting wet patch, rather than penetrate into the dry powder directly underneath it (see Figure 39.5).

The above discussion is for drop penetration into a stationary powder bed. Drops impacting and penetrating into moving powders show more complex behavior. In fluid bed granulation, the fluid slowly flows outwards, and the powder layer is slowly built up by collisions between the wet outer surface of the drop or wet agglomerate and the agitated dry powder [19]. Fluid flow and nuclei formation kinetics are still controlled by the same fluid properties as shown in equation 39.4 but the rate of powder addition to the exterior surface is an additional factor in the kinetics [19]. Growth will continue until the saturation of the agglomerate decreases to the point that no further liquid can reach the powder surface. This saturation limit was defined as the "wetting saturation" S_w and determines whether additional growth will occur (see Figure 39.6).

39.2.1.2 Dimensionless Spray Flux Dimensionless spray flux [9, 13] considers the granulator spray zone and the flux of drops landing on the moving powder surface. The derivation of spray flux is straightforward [9] and is not intended to be equipment specific, although it has been most frequently applied in mixer granulation.

During the liquid addition stage of the granulation process, the powder surface is moving beneath the spray with a velocity v underneath a spray of width W at the powder surface. Therefore, the area of dry powder passing beneath the spray nozzle per second is vW. Each drop hitting the powder surface in the spray zone will leave a "footprint" as it wets into the powder. The number of drops hitting the powder surface per unit time can be calculated by dividing the total liquid flow rate by the volume of an individual drop. Assuming that each drop lands separately on the surface, without overlapping with any other drops, the total wetted area created per unit time can be estimated by multiplying the

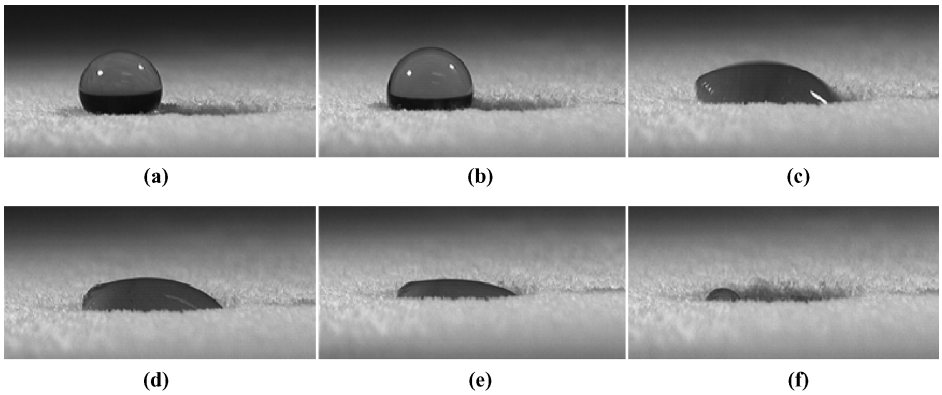

FIGURE 39.5 Penetration of a drop of PEG400 ($\mu = 120$ mPa s) into prewetted lactose 200 mesh powder. The footprint of the previous drop is visible to the right of the added drop (separation distance of 3 mm). (a)Impact; (b) 4.05 s after impact; (c) 5 s; (d) 5.02 s; (e) 12.06 s; and (f) 51.6 s [14].

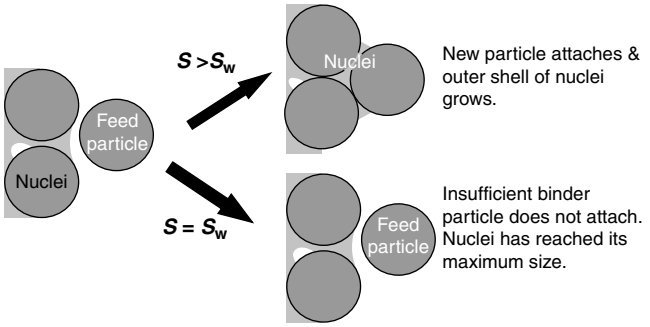

FIGURE 39.6 Nuclei growth in a fluid bed via growth of the outer nuclei shell continues, provided the agglomerate saturation is higher than the wetting saturation limit S_w (adapted from Ref. 19).

number of drops being added per second by the area each drop will occupy when it lands on the powder surface. Dimensionless spray flux is then defined as the ratio of the rate at which wetted area is created by the incoming droplets compared to the total area of dry powder passing through the spray zone [9]:

$$\Psi_a = \frac{\dot{a}}{\dot{A}} = \frac{3\dot{V}}{2\dot{A}d_d} \tag{39.5}$$

The dimensionless spray flux is a measure of the density of drops falling on the powder surface. Physically, $\Psi_a = 0.1$ means that ~10% of the powder surface will be wetted per pass through the spray zone. At low spray flux ($\Psi_a \ll 1$) drop footprints will not overlap and each drop will form a separate nucleus granule. The size of the nuclei will be directly proportional to the drop size [8, 20]. As Ψ_a increases, the fraction powder wetted also increases, although the relationship is linear only at low Ψ_a values. At high spray flux ($\Psi_a \sim 1$) the spray rate is high compared to the rate of dry powder entering the spray zone and the drops significantly overlap each other as they land on the powder bed. Spray flux $\Psi_a \geq 1$ means that the incoming droplets will theoretically cover 100% of the dry powder passing beneath the nozzle, assuming no drop overlap occurs [9]. At this value, the nuclei formed will be fragments of a much larger sheet of wet powder and will bear little relationship to original drop size. Good granulation can still be achieved provided that the shear forces during granulation are large enough and uniform enough to be effective. In pharmaceutical granulation, these conditions usually also consolidate the granules leading to lower porosity granules with slower dissolution. The process is illustrated schematically in Figure 39.1.

Note that $\dot{A}$ is a dynamic quantity, defined as the outer perimeter of powder sprayed per second (m^2/s) and is not equivalent to static footprint spray area, A. The difference between the static footprint area of the spray and the dynamic area flux is illustrated schematically in Figure 39.7 for several cases of varying powder velocity.

The impact of Ψ_a on nuclei formation has been studied in both mixer granulators [11, 17, 21, 22] and externally on a simplified moving power bed [9, 23]. To eliminate the effect of granule growth, the nuclei size distribution was measured after a single pass of the powder through the spray zone [9]. The results clearly show that at low spray flux ($\Psi_a < 0.2$) the nuclei size distribution is quite narrow. As spray flux increases, the distribution broadens as agglomerates begin to form. At very high spray flux ($\Psi_a > 1$), the spray zone has become a continuous cake and the nuclei distribution bears no resemblance to the drop distribution. Further, when the spray flux is low, changes to the spray drop distribution are directly mapped onto the nuclei size distribution [9].

The dimensionless spray flux parameter is intended to capture the major effects of drop overlap in the spray zone on the nuclei distribution as simply as possible, to encourage its use as a scale-up parameter. The derivation contains several major simplifying assumptions. First, the spray is assumed to consist of mono-sized drops. Second, the spray flow rate is assumed to be uniformly distributed over the entire spray area. This is rarely true in industrial applications, as generally, the flow rate is higher in the center of the spray area than at the sides [7, 24]. The theory has been developed and validated for the case of a completely dry powder entering the spray zone. In practice, this is true only for the very initial stages of the granulation process. As spraying progresses, a mixture of dry powder and previously formed nuclei and granules will pass through the spray and will be rewetted, which will affect the final size distribution for some fluids [14].

Finally, the derivation ignores the fact that the nucleus size is always larger than the drop size. During spraying, two drops may land close to each other but without touching. As the liquid penetrates into the powder, the larger nuclei may grow and touch each other, causing coalesce of the nuclei even when the spray drops landed separately. Wildeboer et al. [13] extended the theory and modeling to account for the effects of drop size distribution, nonuniform spray density, and for probability of coalescence due to nucleus spreading. Nucleus spreading is described by the nucleation ratio K, which can be defined on either a volume basis—that is, the ratio of the nucleus volume to the drop volume, K_v [19]—or on an area basis where K_a is the ratio of the projected area of the drop (a_d) to the nucleus (a_n) [13].

Where a is the projected area of the nucleus (a_n) and drop (a_d). Typical values for K_v range between 3 and 30 or higher [18, 19, 23, 25, 26]. The probability of a single drop forming a single nucleus is, therefore, related to the dimensionless nucleation number, Ψ_n [13]:

$$\Psi_n = K_a \frac{3\dot{V}}{2wvd_d} \tag{39.6}$$

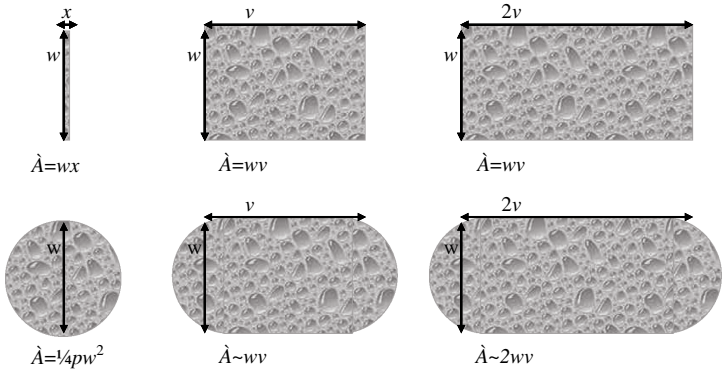

FIGURE 39.7 Relationship between the spray area of the nozzle, A, and the dynamic spray area $\dot{A}$ for a line spray. Upper case shows a line spray and lower case shows a circular spray. Case (a) represents the static spray case where there is no powder motion; case (b) shows the area flux of powder beneath the nozzle for powder moving at v m/s; and case (c) area wetted by the spray for powder moving at $2v$ m/s.

The dimensionless nucleation number Ψ_n differs from the original spray flux Ψ_a by the factor K_a, which accounts for the degree of nucleus spreading. Equation 39.6 has been used to model the nuclei distributions in the spray zone over a range of Ψ_n [13], accounting for nonuniform sprays and nucleus spreading and coalescence. At a given value of the dimensionless nuclei number Ψ_n, the density and size distribution of the nuclei formed on the surface is constant, that is, the final value of Ψ_n is the sole determinant of the final nuclei size distribution (Figure 39.8).

Assuming complete spatial randomness, spatial statistics can be used to derive an analytical solution for both the fraction surface coverage and fraction of agglomerates formed [12]. Under these conditions, the drops landing randomly on the target area are described by a Poisson distribution. The fraction of the surface covered by drops in a single pass through the spray zone is given by [12]

$$f_{\text{covered}} = 1-\exp(-\Psi_a) \tag{39.7}$$

The fraction of nuclei formed from n drops is given by

$$f_n = \exp(-4\Psi_a)\left(\frac{(4\Psi_a)^{n-1}}{(n-1)!}\right) \tag{39.8}$$

Thus, we can calculate the number of single drops, not overlapping with any other drops, and by difference, the number of agglomerates [12]

$$f_{\text{single}} = \exp(-4\Psi_a) \tag{39.9}$$

Equation 39.8 can be used to estimate the initial nuclei size distribution as a function of spray flux for mono-sized drops. Figure 39.9 shows the nuclei distributions predicted by equation 39.8 at a range of spray flux values for 100 μm mono-size drops. As the spray flux increases, a higher percentage of nuclei are formed from multiple drops, creating a larger and broader nuclei size distribution. However, prediction of the bimodal nuclei distributions that form at

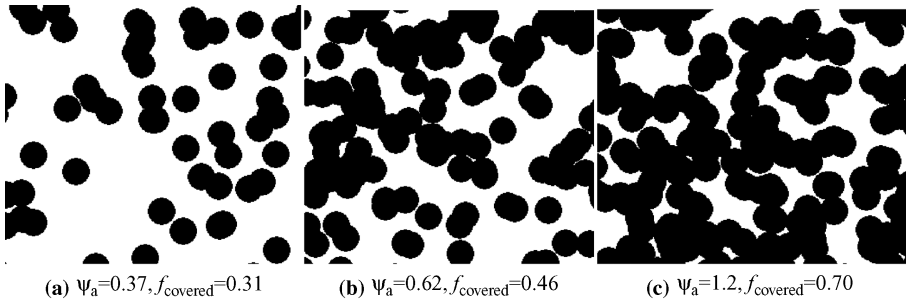

FIGURE 39.8 Monte-Carlo simulations of spray flux.

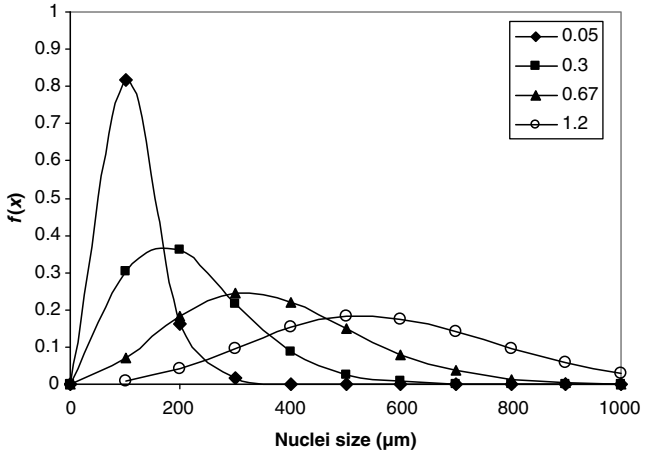

FIGURE 39.9 Nuclei size distributions predicted by equation 39.9 at a range of spray flux values assuming 100 μm monosized drops.

higher spray flux [27] appears to require a more sophisticated modeling approach incorporating overlapping drop size distributions.

Practical application of dimensionless spray flux requires measurements of the drop size distribution and powder velocity, and spray distribution for Ψ_a. Spray distribution is the easiest of the three parameters to measure (e.g., see Ref. 24), and laser diffraction and/or Doppler analysis of spray nozzles is widely available for drop size characterization. Currently, the most challenging parameter in Ψ_a to measure in real granulators is the powder velocity, and this is discussed separately in Section 39.3.2. Drop size in a spray is a strong function of the distance from the nozzle, so the measurements of drop size must be taken at the approximate distance where the spray intersects the bed. This distance usually increases as the granulator scale increases, and varies depending on spray lance design. Increase in the nozzle lance depth causes a reduction in the spray area and hence an increase in spray fluxes. Maintaining a constant nozzle height is important in reducing unwanted variation in granulator performance.

39.2.1.3 Nucleation Regime Map The drop penetration time describes the kinetics of nucleation from a single drop as a function of the material properties in the formulation. The spray flux describes the physical interactions of multiple drops in the spray zone. Together, these two parameters form the basis of the nucleation regime map [10], which describes the optimal conditions for uniform liquid distribution and suggests some ideal conditions for controlled nucleation.

When the drop penetration time is short, the fluid will sink quickly into the powder bed to form a nucleus granule. If no other drops land on top of the sinking drop as it passes through the spray zone, a single nucleus granule will be formed with a size equal to 2–3 times the drop volume (see equation 39.7). If this process occurs for all the drops, the nuclei size distribution will be directly proportional to the drop size distribution. This is known as "drop-controlled nucleation" [10] and occurs at low drop penetration time and low spray flux (i.e., low spray density). As a guide, the spray flux needs to be less than $\Psi_a < 01$ for approximately 2/3 of the nuclei to be formed from a single drop (see equation 39.11).

This "one drop produces one granule" mode of nucleation will not occur with a formulation with the same low drop penetration time, but granulated at a high spray flux. At higher spray flux, the spray density will be too high and the vast majority of the drops will coalesce with another drop on the powder surface. The surface of the powder will be wetted by an almost continuous sheet of liquid, rather than discrete drops. As the powder moves due to agitation, the "caked" powder will be broken and the fragments will be dispersed through the powder. This is the "mechanical dispersion" regime of nucleation [10], where the liquid is dispersed primarily due to powder agitation and shear, rather than by fluid flow and wetting.

If the drop penetration time is much longer, the liquid will remain on the surface of the powder for an extended period of time, in the order of minutes. The constant powder motion means that it is more likely to coalesce with other unpenetrated droplets (see step 3 in Figure 39.2), merge into a section of powder wetted by an earlier drop [14] or roll into depressions in the powder and form rivulets [23]. Even if the drop does not coalesce with other drops, powder agitation and shear will be required to disperse the fluid through the powder to form a nucleus (step 5 in Figure 39.2). Again, this is the "mechanical dispersion" nucleation regime.

These two regimes of nucleation can be summarized using a nucleation regime map (Figure 39.10). The axes of the map are the dimensionless spray flux Ψ_a and the dimensionless penetration time τ_p

$$\tau_p = \frac{t_p}{t_c} \tag{39.10}$$

where t_c is the circulation time for the droplet or nuclei to return to the spray zone. This is currently not quantified due to insufficient understanding of powder flow and circulation patterns in most industrial granulation equipment. In general, the drop penetration time needs to be much faster than the circulation time, and an arbitrary limit of 1/10th of the circulation time ($\tau_p < 0.1$) has been set as the upper limit for drop-controlled nucleation [10].

In the lower left-hand corner of the map is the drop-controlled regime, which occurs at low dimensionless drop penetration time ($\tau_p < 0.1$) and low spray flux ($\Psi_a < 0.1$). In this corner, each drop will generally land separately without touching any other droplets. As soon as either the spray flux or the penetration time increases slightly, the system enters an intermediate region where both wetting and agitation will be

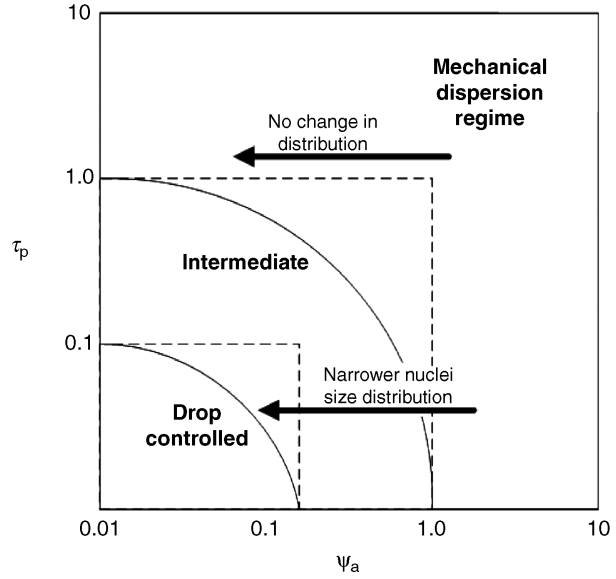

FIGURE 39.10 Nucleation regime map with adjusted boundaries incorporating the drop migration due to rewetting of powder during multiple passes through the spray zone [14]. Dotted lines represent original regime boundaries [10].

equally important in determining liquid distribution and nucleation. As spray flux or penetration time increase further, the mechanical mixing will become the dominant mechanism in nucleation, as the wetting kinetics occur on a much longer timescale.

Understanding which nucleation regime the process is operating in can be extremely useful for understanding how to optimize liquid dispersion and trouble shoot during manufacturing. For formulations with low penetration times, optimizing the spray flux by adjusting the fluid flow rate, the drop size, spray area, powder velocity, etc., will have a significant effect on the process, as it moves from the mechanical dispersion regime toward the drop-controlled regime, crossing the regime boundaries (see lower horizontal arrow in Figure 39.10). As the process nears the drop-controlled regime, the nuclei size distribution will approach the drop size distribution of the spray. Atomization of a fluid is fairly well understood (e.g., [28]) and is therefore much easier to optimize compared to a granulation process. In contrast, when working with a formulation with a long drop penetration time, optimizing the spray parameters to reduce spray flux will have little effect on the nucleation process. Once the drop penetration time is high, it is extremely difficult to achieve drop-controlled nucleation, as the liquid will form a "puddle" on the powder due to either slowly penetrating drops or high spray density. In addition, atomizing a highly viscous fluid can be difficult, and some industrial processes add the fluid as a steady unatomized stream or even scoop in extremely viscous pastes. There is little benefit in atomizing these extremely viscous fluids, as although atomization may assist fluid distribution, mechanical dispersion will still control the overall fluid dispersion process and hence control the nuclei distribution.

Note that granulating in the mechanical dispersion regime implies that efficient mixing and agitation of the powder is required to achieve effective liquid dispersion, and does not automatically mean "poor" liquid distribution. Most mixer granulation processes operate in the mechanical dispersion regime, unless they have been consciously designed to achieve drop-controlled nucleation conditions (see Section 39.3.1 on spray flux scale-up). However, powder flow, circulation patterns, and shear forces in industrial granulation equipment are still poorly understood although there are several groups actively researching in this area [29–33]. Increasing the fluidizing air or impeller speed to improve agitation seems a simple solution, but commonly cannot be done, either due to equipment or process limitations (e.g., fixed speed impellers in mixers, or maximum pressure drop limit in a fluid bed) or due to negative side effects in on the granulation process (e.g., change in granule density and/or growth regime—see Section 39.2.1.2). One way to improve mechanical dispersion is to position the spray in a highly agitated region of the granulator. In a mixer granulator, this can be achieved by placing the spray nozzle either directly over the chopper [34], or shortly before the chopper, so that the recently sprayed powder flows almost immediately into the turbulent chopper zone, rather than completing a 180–270° rotation before being agitated.

39.2.2 Consolidation and Growth

The second mechanism in wet granulation is granule growth (see Figure 39.1) and is inherently linked to both the liquid level and porosity of the granules. It is well known that different formulations show different growth behavior in the same equipment, and that the same formulation can demonstrate changed growth behavior when different granulation conditions or equipment are used. We can think of two extreme models for the process of granule growth, which are as follows:

1. *Growth of Deformable Porous Granules*: The starting force for granule growth and consolidation is a porous deformable nuclei formed by the processes described in Section 39.2.1. The nucleus contains substantial amounts of liquid in the pores but is not necessarily surface wet. This corresponds to a drop size in the spray zone larger than the primary particle size and this model is a reasonable picture of granule growth in high shear mixers.
2. *Near Elastic Granules*: Here we consider the granule to be a nearly elastic particle coated with a liquid binder after it leaves the spray zone. This model is well suited for processes where granules are dried before

they reenter the spray zone and where the liquid drop size is small compared to primary particle size. Thus, this model is often a reasonable description for fluidized bed granulation.

For both models, if we can answer the question: "Will two colliding granules coalesce or rebound?" we will have gone a long way to describing the granule growth behavior. Granule growth regime maps summarize the causes of much of this behavior. Before, describing these models, we first discuss granule strength and deformation, and granule consolidation.

39.2.2.1 Granule Strength and Deformation One way to experimentally study granule strength is through the use of wet granule pellets, which are small wet powder compacts with controlled size, porosity, and liquid content. Pellets are deformed under different conditions (in particular, strain rate $\dot{\varepsilon}$), and the effects of many variables, including binder fluid viscosity and surface tension, particle size, pellet porosity, etc. can be investigated [35–38]. The stress versus time is recorded and the peak stress σ_{pk} indicates the point of failure and converted to a dimensionless peak flow stress Str^* [38]

$$\mathrm{Str}^* = \frac{\sigma_{pk} d_p}{\gamma_{lv} \cos\theta} \tag{39.11}$$

The Str^* data for all the experiments was plotted against the capillary number Ca, which is the ratio of viscous forces to surface tension forces, and proportional to the strain rate $\dot{\varepsilon}$

$$\mathrm{Ca} = \frac{\mu d_p \dot{\varepsilon}}{\gamma_{lv} \cos\theta} \tag{39.12}$$

Figure 39.11 shows this data for spheres. A single relationship can be formed with two distinct regimes [37, 38]. In region 1, the strain rate is low (low Ca) and the peak flow stress is independent of strain rate. In region 2, the higher strain rates applied (high Ca) means that the viscous resistance forces begin to dominate, and the peak flow stress is proportional to the strain rate.

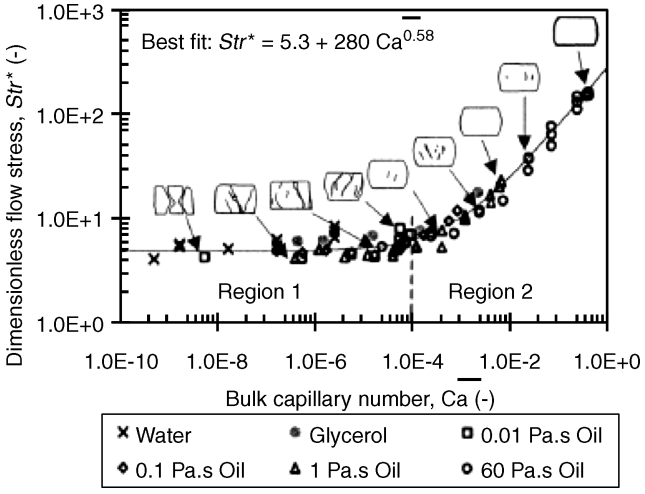

FIGURE 39.11 Dimensionless flow stress versus capillary number [37]. In region 1, the stress is independent of flow rate. At higher strain rates (region 2), viscous forces dominate and the stress is proportional to the strain rate.

Note that this approach confirms that at high enough values of Ca, the peak flow stress (granule dynamic strength) is a strong function of strain rate. As collisions in the granulator are dynamic and collision velocities may vary from approximately 0.1 ms^{-1} to approximately 1 ms^{-1}, this is important. The granule strength should not be measured under static conditions, but rather at strain rates similar to those experienced in the granulator. Granules made from nonspherical primary particles follow a similar behavior to that illustrated in Figure 39.11, but are generally significantly stronger than granules made from spherical model particles. In Section 39.2.3.4, an extended version of the granule strength model is presented which includes effects of primary particle shape and granule liquid saturation.

39.2.2.2 Granule Consolidation A granule is a three-dimensional composite of solids particles, liquid bridges (which covert to solid bridges after drying), and vacant pore space occupied by air. Consolidation is the increase in granule density that results when the primary particles are forced to move closer to each other as a result of collisions between particles. Consolidation can only occur while the binder is still liquid. Consolidation determines the porosity and density of the final granules. Factors influencing the rate and degree of consolidation include particle size, size distribution, and binder viscosity as well as the impeller speed or fluidizing velocity [39–41].

The structure of granules, particularly the proportion and arrangement of the pore space, plays an important role in downstream processing, particularly compaction of the granules into a tablet, and in product performance, especially dissolution of the final solid dosage form [42].

The structure of real granules is complex and has not been able to be studied until the relatively recent development of micro X-ray tomography (XRT) [43–47]. Some examples of the structure of some pharmaceutical granules made in the same equipment from the same formulation at two different mixing conditions are shown in Figure 39.12 and this is an area of continuing research.

Although detailed analysis of the pore size distribution via mercury porosimetry [41, 48, 49] or XRT is possible [42–45], the overall average porosity of the granule has been found to be a very useful parameter in granulation. The overall porosity of a granule ε is defined as the volume fraction of air *within* a granule. Care is needed to avoid confusion between the interparticle voidage between the granules and the intraporosity of the granules (i.e., the internal porosity), both of which affect the bulk and tap density of an assembly of granules. The porosity of the granules generally begins at a

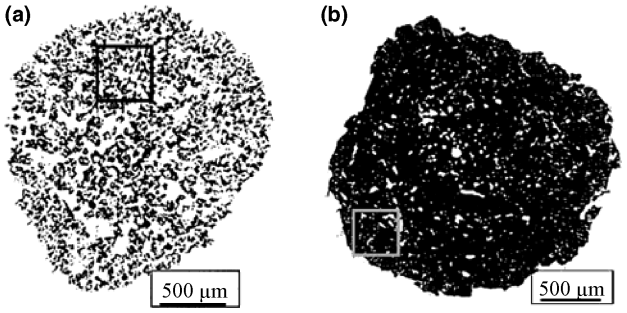

FIGURE 39.12 X-ray tomography images of internal structure of granules produced in a 2 L mixer at different shear conditions (a) 200 rpm impeller and 600 rpm chopper speed $\varepsilon \sim 58\%$ and (b) 600 rpm impeller and 1800 rpm chopper speed $\varepsilon \sim 15\%$ [43].

high value (approximately 50–60%) and decays exponentially as the granulation process proceeds [40] (see Figure 39.13), due to granule deformation and particle rearrangement as a result of collisions with other particles, granulator wall and the impeller or chopper in a mixer granulator. The rate of densification depends on several parameters, but large particle size, smooth round particles, and low-viscosity fluids allow rapid densification [40]. The final porosity reached by the granule, $\varepsilon_{\min}$, is often used to determine the yield strength of the granule. The rate at which granules densify can be related to the granule peak flow stress and the typical collision velocity in the granulator through the Stokes deformation number St_{def}

$$St_{\text{def}} = \frac{\rho_g U_c^2}{2Y_g} \tag{39.13}$$

where ρ_g is the granule density, U_c is the collision velocity, and Y_g is the yield strength of the granule. The yield strength

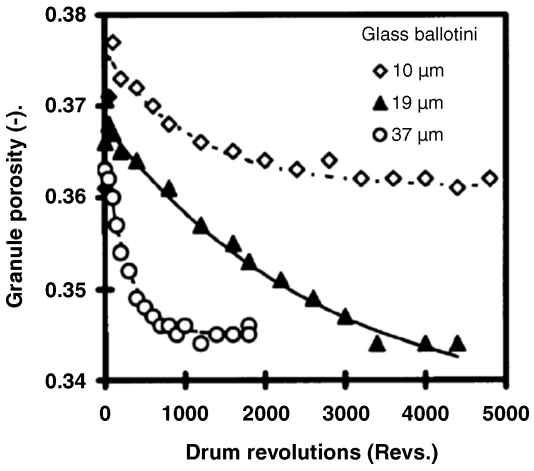

FIGURE 39.13 Exponential decay in granule porosity as granulation proceeds [40].

of the granule is a function of the formulation and the extent of consolidation, and is usually evaluated as the peak flow stress at the minimum porosity $\varepsilon_{\min}$ (see Figure 39.12). The granulation consolidation rate constant k_c is then given by

$$k_c = \beta_c \exp(a.St_{\text{def}}) \tag{39.14}$$

where β_c and a are constant. k_c is the consolidation rate constant for a first-order consolidation equation of the form

$$\frac{\varepsilon - \varepsilon_{\min}}{\varepsilon_0 - \varepsilon_{\min}} = \exp(-k_c t) \tag{39.15}$$

Granule porosity is closely coupled with the granule saturation. The granule saturation s is defined as the proportion of pore space that is occupied by liquid

$$s = \frac{w\rho_s(1-\varepsilon)}{\rho_l \varepsilon} \tag{39.16}$$

where ε is the average granule porosity, w is the mass liquid/mass dry powder, ρ_l is the density of liquid, and ρ_s is the true density of the solid particles.

Four general saturation states have been defined—pendular, funicular, capillary, and droplet (Figure 39.14). There are two ways that the overall saturation of the granule can be increased—the amount of fluid added to the system can be increased, or the granule can be consolidated to reduce the pore space available [50, 51]. During the liquid addition phase of wet granulation, a combination of both processes is most likely occurring. For some formulations, consolidation of the granule will gradually decrease the porosity of the granule until the saturation reaches the droplet state, when the binder fluid will be squeezed to the exterior surface of the granule [24, 52–55]. The sudden presence of fluid at the outer granule surface often induces rapid coalescence and runaway growth of granules [40, 53, 56].

The rate of granule consolidation varies significantly, depending on the properties of the powder and liquid used [39, 40]. The interparticle friction must be overcome so that the granule can consolidate. Interparticle friction is increased by using smaller particle size, as their high surface

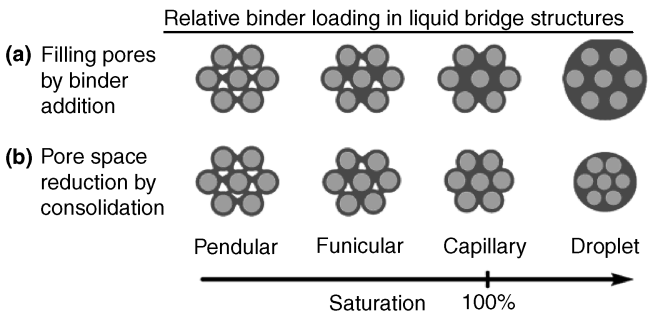

FIGURE 39.14 Granule saturation has four main states, and saturation increases as liquid content increases [50] and pore space decreases.

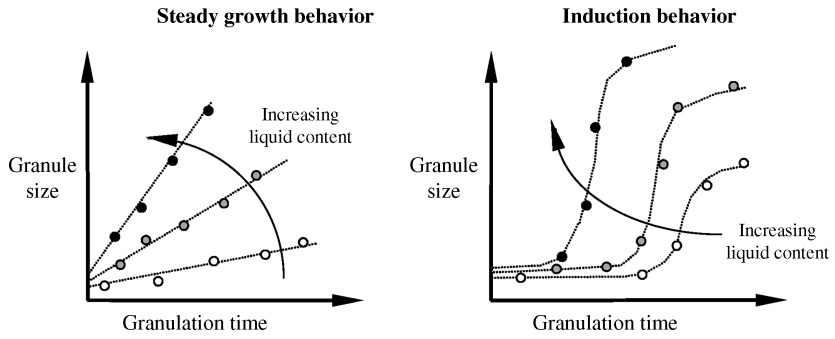

FIGURE 39.15 Two main types of granule growth behavior for deformable granules [52].

area and high number of interparticle contacts provide more resistance to consolidation [39, 40, 57]. Granules formed from coarser particles tend to consolidate more quickly (see Figure 39.12). Viscous binder fluids also reduce the rate of consolidation, as the liquid resists flowing during deformation. However, the presence of fluid also acts as a lubricant and higher liquid content (i.e., saturation) causes the rate of consolidation to increase.

39.2.2.3 Granule Growth Behavior for Deformable Porous Granules There are two main types of granule growth behavior for porous, deformable granules—steady growth and induction growth (Figure 39.15). "Steady growth" occurs when the rate of growth is constant (at a given liquid level). On a plot of granule size versus granulation time, steady growth behavior produces a linear trend. This type of growth occurs in formulations where the granules are easily deformed by the forces in the granulator, and tends to occur when the using coarse powders and low-viscosity fluids [52].

In contrast, "induction growth" occurs when the initial nuclei remain at a constant size for a long period, before very rapid granule growth occurs, resulting in a sudden increase in granule size (Figure 39.15). During the induction period, the granules consolidate and approach some minimum porosity (e.g., see Figure 39.13 for example data) but do not grow in size except through the layering of ungranulated fines. Eventually, the granule porosity can be reduced enough to squeeze liquid to the surface. If there are no ungranulated fines remaining, this excess free liquid on the granules causes sudden rapid coalescence of many granules, and results in the rapid increase in granule size characteristic of an induction formulation.

39.2.2.4 Granule Growth Regime Map for Deformable Granules It is well known that different formulations show different granulation behavior, such as induction versus steady growth. The links between formulation properties and granule growth behavior are summarized in the granule growth regime map [52, 54]. The horizontal axis indicates the granule saturation s, which is a function of the weight fraction of liquid w, and the granule porosity ε (see equation 39.13). On the vertical axis is the Stokes' deformation number, St_{def}, which is the ratio of the kinetic energy experienced by the granules during a collision compared to the yield stress or deformation of the granule (see equation 39.13).

To make effective use of the granulation regime map, we need reasonable estimates of the effective collision velocity U_c (controlled by process conditions) and dynamic yield stress Y (a function of formulation properties). Table 39.1 gives estimates of the average and maximum collision velocities for different process equipment. In high shear mixers, the difference between the average and maximum collision velocities can be very large and the estimates should be taken as indicative.

Let us consider the different growth regimes. First, we should consider a very weak formulation with a low granule yield strength Y_g. For example, coarse sand and water At the very beginning of the granulation process, the saturation s will be low and close to zero and the process in the "dry" free flowing powder section of the regime map, in the upper left-hand corner. As more fluid is added to the process, the saturation increases and we move from left to right across the map. However, in this case the impact forces from collisions are far exceeding the granule strength and the granules shatter as quickly as they are formed, forming a mixture reminiscent of damp sand. Increasing the amount of fluid does not help this, and eventually the system will end up as a slurry, in the upper right-hand corner of the map.

Considering now a formulation, which has a slightly higher granule yield stress Y_g, where granules deform rapidly, but are not shattered. For example, lactose granulated with

TABLE 39.1 Estimates of U_c for Different Granulation Processes

Type of Granulator	Average U_c	Maximum U_c
Fluidized beds	$6U_b d_p/d_b$	$6U_b d_p/d_b\delta^2$
Mixer granulators	$0.15\omega_i R$	$\omega_i R$

Modified from Ref. 58.

water or a low-viscosity binder such as PVP. The St_{def} for this type of formulation could be approximately 2/3 up the St_{def} axis (depending on the granulator conditions, which determine U_c). Initially, at low liquid amounts, the system will be in the nucleation only regime. In this section of the growth map, there is enough liquid to form nuclei but not enough to allow any significant granule growth—the system is water limited. As more fluid is added, the saturation increases and the process cross the regime boundary to enter the steady growth regime, where the granule size increases steadily with time. If we add still more fluid, the granule growth rate will increase further until we reach the rapid growth regime and eventually a slurry (Figure 39.16).

Finally, consider a formulation with a yield stress Y_g, which is able to resist the impact forces experienced in the granulator. A typical pharmaceutical example would be a formulation containing a very fine powder, granulated using a viscous binder fluid such as 5% HPC. After each collision, the granule consolidates slightly, and over time approaches a minimum porosity as shown in Figure 39.13. Initially, when only a small amount of fluid has been added, the saturation will be low and the process will be in the nucleation regime. As the amount of fluid increases, we cross into the induction regime. During the induction period, the granules densify and approach the minimum porosity. If the level of consolidation is enough for force the saturation to exceed 100% (see case (b) in Figure 39.14), the excess liquid that is squeezed to the surface of the granule will cause the granules to coalesce rapidly with the surrounding granules and extremely rapid granule growth occurs.

It is possible to switch the growth behavior from steady growth to induction growth or vice versa. For example, increasing the binder fluid viscosity or decreasing the particle size will slow the rate of consolidation, and move the system toward induction behavior.

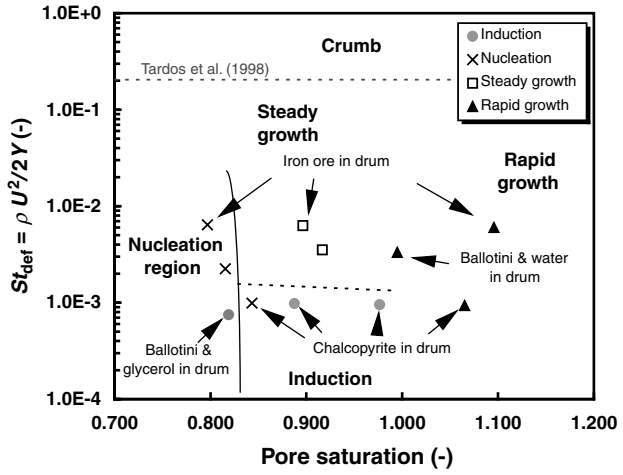

FIGURE 39.16 Granule growth regime map, summarizing the different types of granule growth and the conditions in which they will occur [52].

Pharmaceutical granulation mainly occurs in the nucleation, steady growth and induction regimes, as the final desired granule size is often only 2–4 times the size of the original particles in the formulation. A typical target granule diameter would be 200–400 μm, and the typical size of the particles in the formulation ranges between 50 and 200 μm.

39.2.2.5 Growth Regime Map for Nearly Elastic Granules

For *near elastic granules*, the conceptual model originally developed by Ennis et al. [59] considers the collision between two near elastic granules each coated with a layer of liquid (see Figure 39.17). This work has been summarized in several monographs [58, 60, 61]. In this case the key dimensionless group is the viscous Stokes number St_v

$$St_v = \frac{4\rho_g U_c d_p}{9\mu} \tag{39.17}$$

St_v is the ratio of the kinetic energy of the collision to the viscous dissipation in the liquid layer. Successful coalescence will occur, if St_v exceeds some critical value St^* and we can define three growth regimes, which are as follows:

1. *Noninertial Growth* $[St_{v,max} < St^*]$: The viscous Stokes number for all collisions in the granulator is less than the critical Stokes number. All collisions lead to sticking and growth by coalescence. In this regime, changes to process parameters will have little or no effect on the probability of coalescence.
2. *Inertial Growth* $[St_{v,av} \approx St^*]$: Some collisions cause coalescence while others lead to rebound. There will be steady granule growth by coalescence. The extent and rate of growth will be sensitive to process parameters that will determine the proportion of collisions that lead to coalescence. Varying process parameters and formulation properties can push the system into either the noninertial or coating regimes.
3. *Coating Regime* $[St_{v,min} > St^*]$: The kinetic energy in most or all collisions exceeds viscous dissipation in the

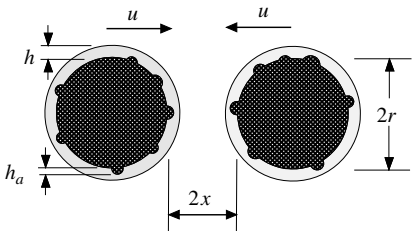

FIGURE 39.17 Two near elastic granules colliding—the basis for the coalescence/rebound criteria [9]. This simple model predicts that granules will grow to a maximum size by coalescence and such behavior is commonly seen in fluidized bed granulation. Note that the key formulation parameters are binder viscosity and particle size, as for deformable granule growth case.

liquid layer. There is no coalescence. Granule growth will only occur by the successive layering of new material in the liquid phase (melt, solution, or slurry) onto the granule.

This simple model predicts that granules will grow to a maximum size by coalescence and such behavior is commonly seen in fluidized bed granulation. Note that the key formulation parameters are binder viscosity and particle size, as for deformable granule growth case.

39.2.3 Breakage

Of the three granulation mechanisms, granule breakage is the least understood. There is no fully general regime map for breakage, although there is an active research effort to develop one. A thorough review of breakage research was published recently [62]. Breakage of wet granules is only important in mixer granulators. Attrition and breakage of dry granules can also occur during fluidized bed drying (and during fluid bed granulation) or during later handling.

The two main approaches to understanding wet granule breakage are to conduct breakage studies of single granules (both wet and dry), or to conduct studies of breakage during granulation within the granulator and granular motion in granulators (including the forces and velocities experienced by the granules). It is important to understand how an individual granule will deform and break under certain conditions. Therefore single granules studies, both experimental and theoretical, can be very useful. Breakage during granulation is usually studied by either analyzing the change in granule size distribution with time, or by using colored tracers.

Granule breakage is a function of the strength of the granule compared to the impact velocity and shear forces experienced by the granules within the granulator. Granules will respond differently under different conditions, and a given granule may break very differently, or not at all. Therefore, granular flow has a large impact on the breakage behavior in the granulating system, but is relatively poorly understood.

It is important to note that the breakage behavior of dry granules is completely different to the breakage behavior of wet granules. We discuss here the breakage of wet granules during the granulation process, which may also be applicable to a wet milling process, but cannot be extrapolated to a dry milling process or any other dry granule breakage process. Dry granule breakage is discussed in detail elsewhere [58].

39.2.3.1 Deformation and Breakage of Single Granules

Deformation and breakage of single wet granules has been studied with high velocity impacts [63], in controlled powder shear [64] and in unconfined compression at varying strain rates [65]. Tardos and coworkers were one of the first groups to study breakage of single wet granules [64]. They performed experiments with individual pellets in a fluidized coquette device, where the shear field applied to the granules was known and carefully controlled. Breakage occurs when St_{def} is greater than some critical value St_{def}^{*} of order 0.2. Here, the granule mechanics were modeled as a Herschel Bulkley fluid and the granule strength is taken as the plastic yield stress under shear. Smith and coworkers [65, 66] extended Iveson's work on granule strength under uniaxial and diametrical compression [35, 37, 38, 67] and showed that in fact the deformation and breakage behavior of single granules is complex. Some formulations show very plastic behavior, while other fail in semibrittle fashion, with propagation of single large cracks through the granule (see Figure 39.18). It is likely that plastic granules may fail

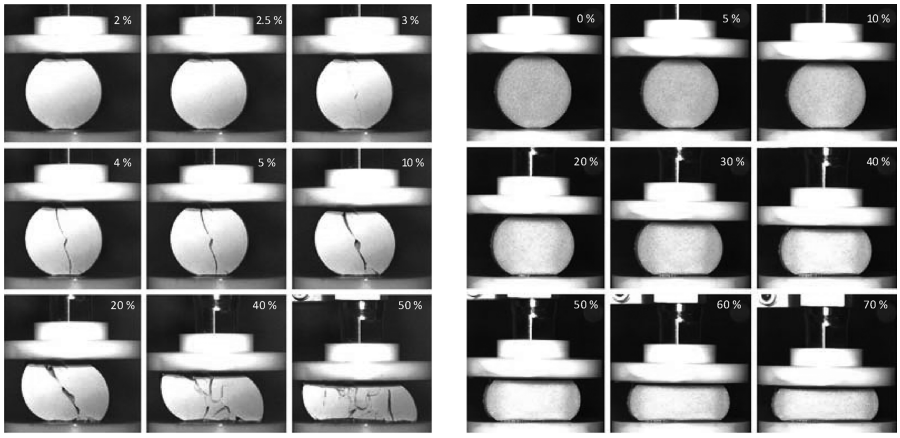

(**a**) Semibrittle behavior (**b**) Plastic deformation

FIGURE 39.18 Extremes of wet granule deformation and breakage behavior in diametrical compression [66].

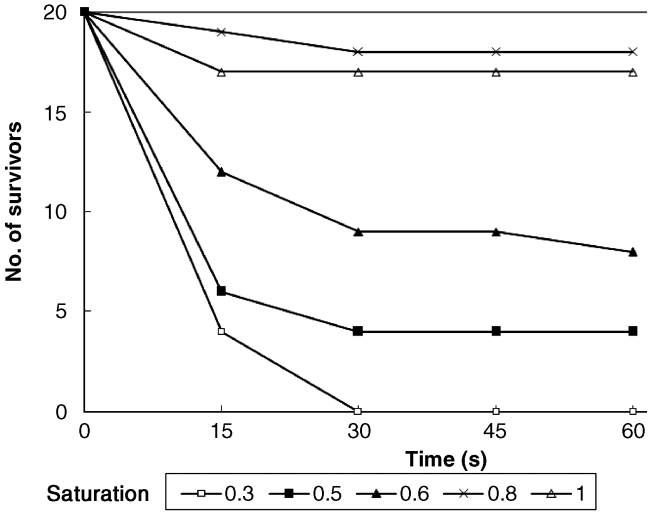

FIGURE 39.19 Breakage of wet granule pellets in a flow field of cohesive sand in a vertical axis mixer granulator (broad size distribution lactose with 1 Pa S silicone oil binder at different liquid saturation values) [70].

by shear and extensional flow in the granulator, while semibrittle granules may break by impact in the impeller zone.

While plastic behavior is more likely to be seen at higher strain rate, there is no general relationship between capillary number Ca and breakage mode. However, granules made from nonspherical particles are both much stronger, and more likely to fail in semibrittle fashion by major crack propagation.

39.2.3.2 Breakage of Granules within the Granulator: Effect of Formulation Properties and Process Parameters

Wet granule breakage has only been identified as a significant mechanism in high shear granulators [26, 62, 65, 68–73]. The problem with fundamental studies using measurements in the granulator is that it is very difficult to deconvolute the effects of breakage from those of nucleation and growth simply by analyzing granule size distributions. To get around this problem, the following two approaches have been taken:

1. Using a small population of well-formed granules or pellets in a flow field of a cohesive, but nongranulating powder such as sticky sand [65, 69, 70] or
2. Using marked tracer granules in a flow field of the same material [26, 68, 72–75].

Figure 39.19 shows examples of the breakage of well-formed pellets with time within a vertical axis mixer granulator [70]. In this case, pellet survival is a strong function of liquid saturation. In general, strong granules (as measured by peak flow stress in uniaxial compression as described above) do not break as readily in the granulator. We can postulate that in the granulator, granules will break if they experience stresses, which exceed their peak flow stress. We can express this as a Stokes deformation number criterion. Breakage will occur if the Stokes deformation number on impact exceeds a critical value [70]

$$St_{\text{def}} = \frac{\rho_g v_c^2}{2\sigma_p} > St^* \tag{39.18}$$

This approach is similar to that used by Tardos and coworkers in the coquette flow rheometer [64]. Figure 39.20 shows that treating breakage data in this way leads to a surprisingly sharp transition from no breakage to breakage at $St^* = 0.2$ for a wide range of formulations.

In similar studies, van den Dries et al. [68] proposed a critical value of $St^* = 0.01$. Closer inspection of the analysis shows that differences in value for St^* are most likely due to differences in mixer geometry and in measuring or estimating the granule strength σ_p and the collision velocity v_c. In their work, Liu et al. [70] combined data from single granule strength measurements [65] with Rumpf's expression for granule strength where both viscous and capillary forces are important, to develop the following expression for granule strength

$$\sigma_p = AR^{-4.3} S \left[6 \frac{1-\varepsilon}{\varepsilon} \frac{\gamma \cos\theta}{d_{3,2}} + \frac{9}{8} \frac{(1-\varepsilon)^2}{\varepsilon^2} \frac{9\pi\mu v_p}{16 d_{3,2}} \right] \tag{39.19}$$

where AR is the aspect ratio of the primary particles, S is the granule pore saturation, ε is the porosity of the granule, $d_{3,2}$ is the specific surface area diameter of the particles, and v_p is the relative velocity of the moving particle inside a granule after impact. The expression explicitly accounts for the effects of primary particle size and shape, liquid binder properties, and liquid saturation. The collision velocity was assumed to be

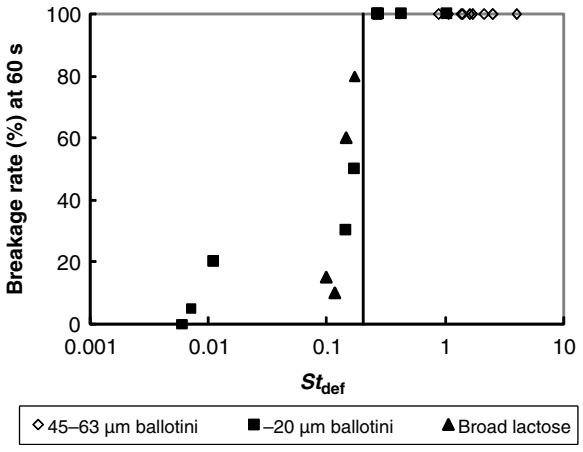

FIGURE 39.20 The extent of breakage at steady state versus Stokes deformation number St_{def} for all the formulations. The vertical line is the St_{def} value of 0.2 [70].

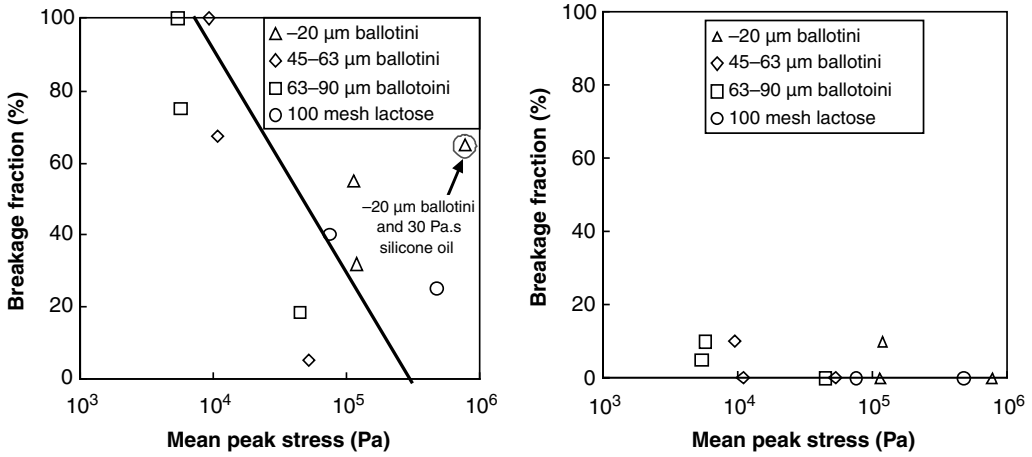

FIGURE 39.21 Breakage fraction of drop formed granules as a function of granule mean peak stress (a) 11° beveled blade at 500 rpm; (b) frictional flat plate impeller at 500 rpm. Modified from [69].

15% of the impeller tip speed. Note this correlation is similar to, although not identical to the Iveson correlation for granule strength (see Section 39.2.2.1). Both predict granule strength increases with increasing strain rate, increasing binder viscosity, and decreasing primary particle size.

Note that the mode of breakage as well as the granule strength may vary with formulation properties. Analysis of granule fragments from breakage shows evidence of significant elongation for some formulations (plastic deformation) and sharp angular fragments for others (semibrittle behavior) [69]. Breakage behavior is similar to that predicted from diametrical compression of single granules.

While this relatively simple approach is fairly general but able to predict the effect of formulation parameters, predicting the effect of changes in equipment parameters is more difficult. In general, increasing impeller speed increases the extent of breakage [26, 71, 73] and this is accounted for by the collision velocity term in the Stokes deformation number. However, breakage is very sensitive to changes in mixer and impeller geometry in ways we cannot yet predict *a priori*. Figure 39.21 shows an example of breakage of single drop formed granules in the same mixer with (a) a two-blade beveled edge impeller and (b) a frictional flat plate at the same impeller speed. For the beveled impeller, there is a reasonable correlation between breakage and granule strength consistent with equation 39.19. (The degree of scatter is due to the difficulty in keeping granule porosity and liquid saturation constant with this method of granule formation.) In contrast, there is *no* breakage using the frictional flat plate.

These results emphasize that breakage is not occurring uniformly in the bed, but rather in a narrow zone near the impeller. This is the reason that granules take time to break in the granulator. Figure 39.19 shows that the pellet granules take up to 1 min to break, even in a small granulator. Figure 39.22 shows an example of velocity fields in roping flow in a two-blade impeller vertical axis mixer. Powder velocity (and therefore applied stress) is very nonuniform with the highest velocities in a small zone near the impeller. As granules circulate in roping flow in the granulator, they will often bypass the impeller zone. Only those granules that enter this zone of high impact and shear stress are likely to break. The size of this breakage zone, and the maximum stresses and collision velocities seen by the granules in this zone will be a strong function of the impeller design.

In mixer granulators, a "chopper" mounted either in the side wall or in the granulator lid, rotates at high speed (e.g., 3000 rpm). This generates a small localized area with very intensive agitation, where breakage could be expected to dominate. The chopper is commonly thought to break up large lumps and granules, particularly at the powder surface (where they are generally located). Although this seems logical, there is no work to demonstrate this—the few pharmaceutical studies that have been performed [48, 77–79] find that the chopper had a very small effect, and that the overall granulation response (e.g., granule size and porosity) is dominated by the impeller speed, liquid level, etc.

39.2.3.3 Breakage of Granules within the Granulator: Effect of Granule Size and Density There are several studies, which show that the breakage probability is proportional to granule size [70, 72, 80]. These studies are consistent with the literature on particle size effects on crushing and grinding. Larger granules are more likely to have large pores or flaws which increases their probability of semibrittle fracture [80]. Consolidated, dense granules are well known to be stronger. An analogy between the granule growth regime map and breakage behavior has been postulated, where three "exchange mechanisms" have been proposed

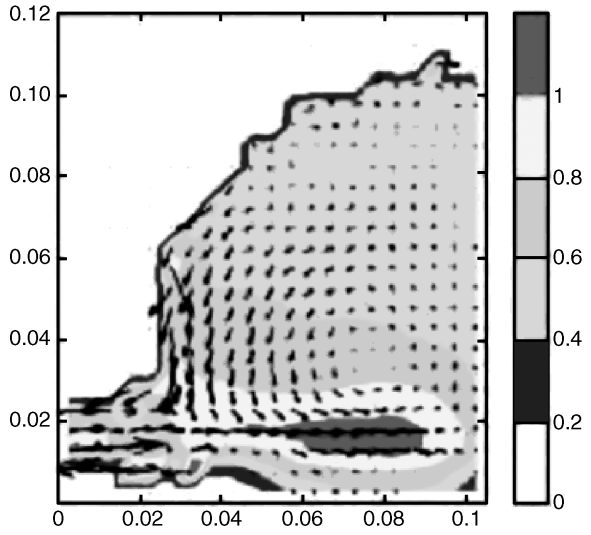

FIGURE 39.22 Powder velocity field during pseudoroping flow in as two-blade impeller vertical axis mixer measured using positron emission particle tracking [76].

to resemble three growth regimes, and linked to the type and rate of material transfer between granules [75].

Colored tracer granules have been used to follow breakage as a function of granule size. Three sizes of colored tracer granules (∼200, 500, and 1000 μm) were added to a granulator while it was running. Samples were taken as a function of time, and the proportion of colored material in each size fraction was analyzed. The largest granules break at a higher rate than smaller granules, as shown in Figure 39.23 [72]. They also investigated the breakage rate of tracer granules that had been granulated for different times, before being removed and added to the running granulator. Younger, newly formed tracer granules broke at a faster rate than tracer granules that had been granulated for a longer period,

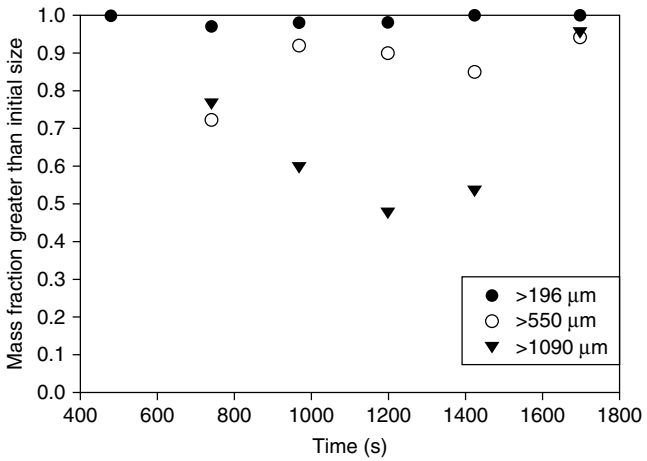

FIGURE 39.23 Coarse granules (>1190 μm) break at a faster rate than smaller granules [72].

allowing plenty of time for granule consolidation [72]. Granule strength, and hence granule breakage rates, have been shown to be quite heterogenous [74]. In some cases, the color distribution of the granules has become almost uniform within approximately 2 min [26, 68, 72], although this will not be true for all formulations or all granulation conditions.

39.2.3.4 Aiding Controlled Granulation via Breakage Breakage of wet granules during the granulation process is not necessarily detrimental. In pharmaceutical granulation, the formation of large granules is generally undesired, and size-preferential breakage of coarse granules [72] helps keep the proportion of coarse granules low.

Breakage can also occur early in the granulation process, in parallel with nucleation, and can assist in distributing the liquid evenly throughout the powder. The mechanical dispersion nucleation regime (see Section 39.2.1.3) requires breakage to disperse the wet clumps of binder fluid through the powder. Newly formed granules (i.e., nuclei) are easier to break than older granules, due to their relatively high porosity [72]. This mechanism of liquid dispersion via breakage of nuclei is called "destructive nucleation" [26] (Figure 39.24). The initial interaction of the drop either in a fluid bed (via layering of the powder on the exterior of the drop) or during the drop penetration process (more relevant to mixer granulation) forms a primary nuclei with a saturation gradient—the saturation decreases as you move from the inner core of the granule to the exterior surface. The large, low porosity, weak primary nuclei is broken into smaller and stronger secondary nuclei, which form starting materials for coalescence [26]. Tracer studies showed that the proportion of primary nuclei that survive decreases as the impeller speed increases [26, 68], and consequently the colored tracer fluid became more uniformly distributed both between granules and within granules. This effect may be smaller for other formulations and equipment (Figure 39.23).

The final stage in destructive nucleation shows a balance between coalescence and breakage, which implies a stable maximum granule size. This idea was applied, together with several other ideas, to produce a well controlled granulation which required only a single parameter—the impeller speed—to be adjusted on scale-up [81]. Note that because the kinetics of breakage in time scale to a typical pharmaceutical granulation (1–5 min), this "steady-state" approach will require longer granulation times for stable results. This work is described in more details in Section 39.3.4.

39.2.3.5 Summary Comments While much is still to be done in the area of wet granule breakage, we can draw some useful conclusions:

1. Approaches used to measure or estimate the effect of formulation properties on granule strength for the

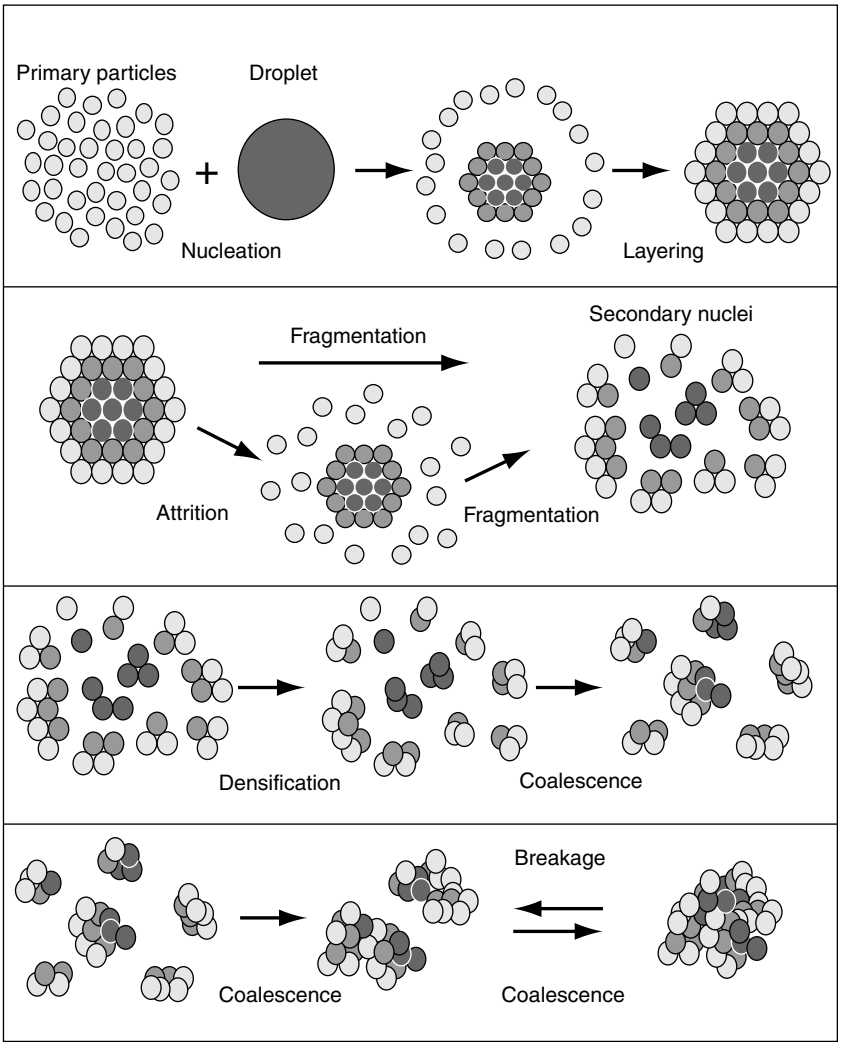

FIGURE 39.24 "Destructive nucleation" where nuclei undergo breakage [26].

purposes of understanding granule growth are also applicable to breakage studies. Remember, however, that changing the formulation can change the mode of breakage (plastic of semibrittle) as well as the yield stress.

2. In the granulator, granules will break due to some combination of shear and impact in a relatively small region near the impellers. Granulator and impeller geometry have a very strong, but difficult to predict effect on the rate and extent of breakage.
3. A simple Stokes deformation number criterion (equation 39.18), can be used to predict whether breakage will occur in a granulator of well defined geometry and to predict the effect of formulation effects and impeller speed on wet granule breakage in the granulator.
4. Granule breakage will occur more easily for large, low-density granules.
5. Breakage can sometimes have a positive effect in wet granulation to aid liquid distribution and limit maximum granule size.

39.3 SCALE-UP

39.3.1 Spray Flux Scale-Up

Dimensionless spray flux provides a good basis for scale up of the spray zone conditions to maintain good nucleation and equivalent liquid distribution conditions. However, maintaining constant spray flux on scale-up can be quite challenging (see also discussion in Ref. 50). The most common scale-up approach is to maintain the same solution addition time, which means that the flow rate through the nozzle increases and therefore spray flux also increases dramatical-

ly. The larger spray width and larger drop sizes at higher flow rates are not usually enough to compensate for this. An alternate approach of maintaining the same flow rate (and drop size, if an identical nozzle tip), but this causes the total batch time to increase in proportion to the batch size. Assuming that liquid level is high enough to produce a granule saturation higher than the nucleation regime limit [52, 54], then the growth and consolidation will be affected due to the longer processing time.

In addition, the powder surface velocity in a mixer granulator generally decreases as the granulator scale increases [21], particularly if the impeller has only two fixed "high" and "low" settings which are usually scaled to maintain equivalent impeller tip speed, rather than equivalent powder agitation and mixing. Lab scale mixer granulators display vigorous mixing and tend to operate in the "roping" regime, while at manufacturing scale the powder agitation is much less efficient, and spends at least part of the time in "bumping" flow [11, 21, 33]. Increasing the impeller speed to maintain an equivalent powder surface velocity also increases the impact and shear forces experienced by the granules. The higher force increases the consolidation rate and shifts the system upwards on the granule growth map (i.e., St_{def} increases). If this upward shift results in the system crossing a regime boundary, a fundamental shift in granulation behavior will occur as the system moves into a different granulation regime.

Table 39.2 gives an example of spray flux changes during scale-up from a 10 kg to a 50 kg batch, where 25% of granulating fluid is added at 0.5 L/min over 5 min. Initially, the calculated spray flux $\Psi_a = 0.36$, which is above the drop-controlled nucleation regime. In the first approach, the spray rate increases to 2.5 L/min to maintain the equivalent granulation time of 5 min and the impeller speed of 108 rpm is scaled using the common "tip speed" scaling rule [21]. The decrease in powder velocity and the increase in spray rate creates an increase in spray flux to $\Psi_a = 1.08$. In the second case, the spray rate is maintained at 0.5 L/min but the spray delivery time is increased from 5 min to 25 min. This is not commonly done, due to fears of significant changes in granule growth and consolidation, which may be unfounded (see Section 39.3.4). In this case, the spray flux remains almost constant at $\Psi_a = 0.38$. The spray flux could be reduced further by increasing the impeller speed, or by adding multiple nozzles.

TABLE 39.2 The Effect of Scale-Up on Spray Flux Ψ_a in Fielder Mixer Granulator

Scale-Up Approach	Base Case	Constant Spray Time	Constant Spray Rate
Batch size (kg)	10	50	50
Flow rate (L/min)	0.5	2.5	0.5
Spray time (min)	5	5	25
Drop size (μm)	200	350	200
Spray width (m)	0.25	0.3	0.3
Impeller speed (rpm)	216	108	108
Powder velocity (m/s)	0.7	0.55	0.55
Spray flux, Ψ_a	0.36	1.08	0.38

Multiple nozzles are the only way to maintain spray flux independently of granule growth and consolidation rates. This is well known in fluid bed granulation scale-up [82–84] but has not been applied to commercial mixer granulators. A four nozzle spray manifold was designed for a 300 L mixer granulator [85]. The increased liquid distribution area and reduced flow rate per nozzle reduced the spray flux and can result in reduced lump formation [85]. An alternate method to maximize liquid dispersion in the spray zone is to place the spray nozzle directly over the chopper, where the turbulent powder flow and strong localized shear forces disperse the fluid effectively, even in the mechanical dispersion regime [34].

39.3.2 Scale-Up of Powder Flow Patterns in Mixer Granulators

Mixer granulators are often called "high shear" granulators, and until recently it was assumed that the impeller was able to effectively agitate the powder bed during operation. Powder velocity measurements can be performed using high-speed video cameras and image analysis [11, 21, 22], which generally measures the tangential component of the powder velocity, although the velocity also varies radially. More sophisticated analysis using positron emission particle tracking (PEPT) technology has also been performed in several mixers [31, 86–89] and shows these trends in much greater detail although the data currently available is limited to lab-scale granulators. Experimental PEPT data for powder flow in larger scale equipment is currently being generated.

Two distinct types of powder flow have been observed in high shear mixer granulators [11]. At low impeller speeds, the powder surface remains horizontal and the bed "bumps" or "shunts" [90] up and down as the impeller passed underneath. The surface velocity was approximately an order of magnitude lower than the impeller tip velocity. As the impeller speed increases, the powder surface velocity increases linearly although there was still little vertical interchange of material. After increasing the impeller speeds above a critical point, a vortex appears and spiraling "roping" [11] or "torroidal" powder flow is observed [73]. In the roping regime, the surface velocity is independent of impeller speed [11, 73] and material from the bottom of the powder bed is forced up the vessel wall before tumbling down the vortex in the center of the powder flow. In all observed powder flows in mixer granulators, the powder velocity is at least one order of magnitude lower than the impeller tip speed [9, 21, 73, 88].

An industrial study of powder flow patterns and surface velocity was performed in a series of Fielder mixers (25, 65, and 300 L) as a function of impeller speed [21]. When running the 300 L granulator at the standard "low" speed setting of 180 rpm, the powder was stagnant approximately 1/3 of the time [21]. Changes in mixer geometry and fill level could significantly change the powder velocity at a given impeller speed. They also measured powder velocity during granulation, and found that the surface velocity gradually increases as granulation proceeded. The powder flow pattern also changed during granulation, shifting from bumping flow during dry mixing to roping flow during granulation [21]. Powder velocity during the dry mix stage has also been shown to vary between lots of API for a high drug load formulation [22]. The measured powder surface velocity for three batches containing different lots of the API varied between 0.64 and 0.95 m/s. This variation was presumed to be due to lot-to-lot differences in drug properties, although establishing the causal link between drug properties and powder flow is an area requiring further investigation.

In fluidized beds, the fluidizing airflow is always adjusted to maintain adequate fluidization of the powders. It would be unthinkable to attempt to scale-up a fluidized bed and select a set of operating conditions which did not fully fluidized the bed—yet we routinely scale-up mixer granulators in exactly this way. There are three main approaches to scaling powder flow in a mixer granulator which can be summarized by the following equation [33]:

$$ND^n = \text{constant} \tag{39.20}$$

where N is the impeller speed (rpm), D is the impeller diameter (m), and n is a scaling index. The most common impeller scaling approach is to maintain tip speed, where $n = 0.5$ [47, 91–93]. An alternate approach is to use Froude number ($\text{Fr} = N^2D/g$), which is commonly used to scale up fluid mixing by maintaining the ratio of centrifugal to gravitational forces [11, 91, 94, 95]. In this case, the scaling index in equation 39.13 is $n = 1$. More recent work used calibrated tracer pellets with a known yield stress to measure the average shear stress experienced by a granule during granulation. Scale-up studies showed that for a series of geometrically similar Fielder granulators, the scaling index n varied between 0.8 and 0.85 [33] depending on the height to diameter ratio, fill level and impeller style used in each case. The "equal shear" scale-up criterion is the subject of ongoing research [96, 97].

In addition to the impeller speed criteria outlined above, other scaling criteria include maintaining swept volume [79], constant energy per unit mass [98], and power number [99].

39.3.3 Granule Growth Scale-Up

It is important to stay within the same granule growth regime (see Figure 39.15) during scale-up to avoid dramatic changes in growth behavior. This is unfortunately easier said than done. The forces applied to the powder mass must remain similar; otherwise the system may shift vertically on the regime map, typically into or out of the induction growth regime. For fluid beds this implies maintaining similar fluidizing conditions and maintaining an equivalent excess gas velocity. For mixer granulators, the maximum impact (e.g., impeller and/or chopper tip speed) may need to be maintained if the granulation is controlled by direct impeller impacts, or perhaps the overall roping flow field to maintain equivalent shear. In some cases, these requirements may directly contradict the requirements needed to maintain equivalent nucleation conditions.

Shifting vertically on the regime map due to a change in the overall force applied to the granulation also implies that the granule porosity and/or structure will also shift, and this is usually undesirable as granule porosity is often shown to be directly linked to the dissolution rate of the granules, capsules, or tablets [42, 100]. Changing the porosity also changes the overall saturation of the granules, which also means that a change in the granule porosity moves the process both vertically and horizontally on the growth regime map. A change in porosity ε and the subsequent change in granule saturation s means that the granule size will change, even though the amount of liquid added to the batch (w in equation 39.11) remains constant. Typically, pharmaceutical process engineers concentrate on keeping the amount of liquid added to the batch constant. In actual fact, the granule saturation is the key factor in controlling granule growth but in the future we hope to see saturation being calculated at each stage of the scale-up process. Currently, the lack of knowledge of porosity changes meaning that the amount of liquid added to the batch is frequently adjusted from compensate for the changes in growth after scale-up.

39.3.4 Scale-Up Case Study: Steady-State Granulation

"Pseudosteady-state granulation" (also called one-dimensional granulation) is a recent approach to wet granulation which resulted in improved control of granule size, properties, and scale-up without any loss in product performance [81]. During a typical 5–25 min pharmaceutical granulation process, there are multiple dynamic subprocesses occurring including liquid distribution; dissolution and hydration of excipients such as lactose, MCC, and dry binders; granule growth; granule consolidation; granule breakage; and the overall granulator flow pattern and shear (particularly the transition between bumping and roping flow). Generally when the batch is stopped, each of these subprocesses is stopped abruptly, well before an equilibrium is reached. Each subprocess has its own characteristic timescale, and it is *impossible* to halt in *all* of these dynamic subprocesses at the *same* point at each scale, and this is why the granulation performance shifts as during scale-up.

An ideal granulation process would allow complete control of liquid sizes in the granulator, without the need for dry milling [81]. The ideal process would allow all the transient subprocesses to reach a repeatable, controllable equilibrium end point, and produce a narrow size distribution of granules between 200 and 500 μm with complete control of the granule size by adjusting only the liquid level. This would involve operating at a low spray flux by using a slow spray rate; a long granulation time to ensure that all complete dissolution/hydration of all the excipients; ensuring roping flow behavior during the entire process; and using some wet massing time to ensure that an equilibrium can be achieved. Vonk et al. [26] showed that an equilibrium granule size and saturation should exist where the rate of granule growth is exactly balanced by the rate of granule breakage (see lower diagram in Figure 39.18). As the entire granulation batch converges toward equilibrium point, the granule size distribution and saturation distribution will also converge. This "steady-state" granulation point should also be scale-independent [81].

To demonstrate steady-state granulation, Michaels et al. [81] granulated a standard lactose-MCC based formulation in a 2 L high shear mixer granulators using "conventional" conditions (40% fluid sprayed over 5 min) and "steady-state" conditions (28% fluid sprayed over 15 min plus up to 20 min wet massing time). The long granulation time caused the initial batches to heat up, creating new transients in evaporation and rheology, so the standard mixer cooling jackets were used to minimize the temperature rise in the batch. The granules produced by the steady-state process were typically 200–300 μm with a narrow size distribution with no granules larger than 1 mm. The final particle size distribution was a function only of the final liquid saturation and shear stress in the agitated wet mass. The granulating fluid level (ratio of liquid added to dry powder ingredients) became a material variable rather than a process variable, that is, scale-independent. In contrast, the conventional granules had a very broad distribution with more than a third of the granules above 1 mm, thus requiring the use of a dry mill.

Scale-up of the steady-state granulation process involves only one process variable: scale-up of the shear stress, controlled by the main impeller speed. Scale-up trials were conducted at 2, 25, and 300 L scale, using the "equal shear" scale-up correlation ($n = 0.8$ in equation 39.15) between shear stress and main impeller speed [33]. The granule size distributions were unimodal and centered at 200–300 μm depending on the liquid level, and the need for a milling step to control the granule size was eliminated [81]. The entire size distribution was matched "right first time" with only a single batch performed at 25 and 300 L (see Figure 39.25). This exact matching of the entire size distribution was repeated multiple times, over three different liquid levels (24%, 28%, 32%) and at two different impeller speed (shown as low, medium, and high shear on the x-axis) at each scale. Although the total granulation process time was far longer than normal (15 min solution delivery plus 20 min wet massing time), the lower liquid level (~28% compared to 45% for the same formulation granulated using a standard approach) and the small, uniformly size granules meant that the drying time was significantly shorter, resulting in the same

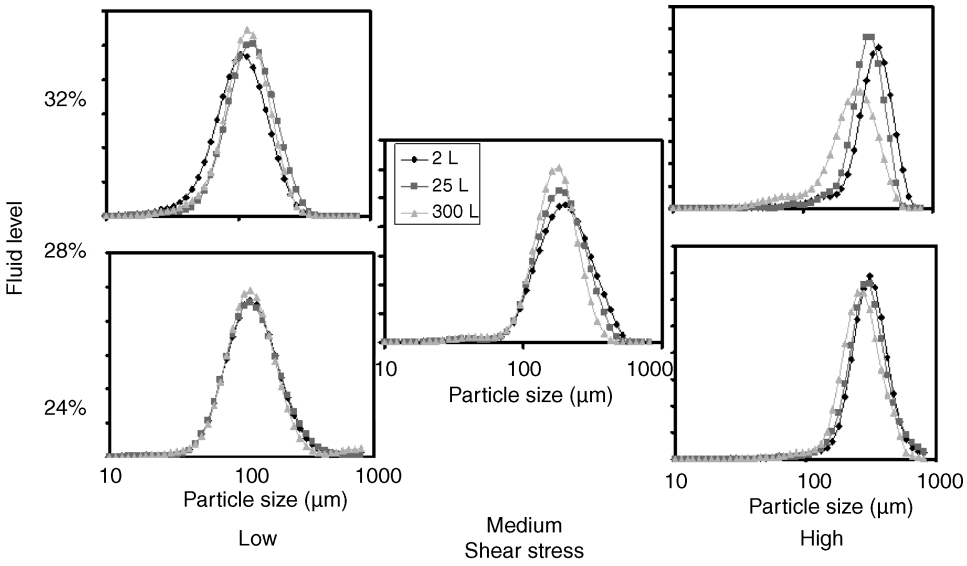

FIGURE 39.25 Particle size of dry, unmilled granules manufactured at 2, 25, and 300 L scale. Data shown for three fluid levels (24%, 28%, and 32%) and three shear stresses (low, medium, and high impeller speeds).

overall cycle time at production scale. In addition, the dissolution and compaction of these granules was unaffected, contrary to conventional opinion that such dense granules would fail to meet physical tablet specifications and drug release specifications. This highlights the surprisingly simple opportunity of using the steady-state granulation approach to scale up pharmaceutical formulations. The approach has also been successfully used for granulation of detergents in a fluid bed granulator [101].

39.4 FUTURE DIRECTIONS

There are several areas where the existing knowledge of granulation is currently insufficient—powder flow including the shear rates and collision rates experienced by the granules is one area, and a better understanding of the granule breakage mechanism is another. Both of these areas are the focus of several international groups. Areas particularly relevant to the pharmaceutical industry are the granulation behavior of multicomponent powder blends, and understanding how to obtain the most uniform drug distribution possible across all granule size fractions. The behavior of hydrophobic drugs in granulation can also be quite surprising [46, 102] and warrant further effort.

In future, the granulation process—that is, operating conditions for a given formulation to produce granules with a prespecified set of properties—will be designed entirely in advance using dimensionless groups and regime maps. Selection of robust process conditions based solely on theoretical considerations has already been demonstrated [81]. The existing knowledge provides valuable guidance for trouble-shooting process problem and estimating the process risk of atypical events.

Pharmaceutical granulation is also evolving—continuous granulation is now under serious development [103, 104] and is clearly a strong future direction of pharmaceutical granulation. Continuous granulation will also require a new effort to develop online process control and analytical technology—particularly for granule size and porosity. The technology for online and at-line granule size measurement already exists but is currently used only sparingly [81, 105], in part due to industry conservatism about applying a novel particle size measurement. The development of real process control will most likely also impact on more traditional batch granulation. Other improvements, including the use of foam to distribute the binder fluid instead of a spray [106–108] are also likely to expand the range of process options available during pharmaceutical wet granulation. The new engineering-focused approach to pharmaceutical granulation is leading to vast leaps in our understanding of the granulation mechanisms and the future direction is the gradual merging of granulation science and industrial know-how.

REFERENCES

1. Iveson SM, Litster JD, Hapgood KP, Ennis BJ. Nucleation, growth and breakage phenomena in agitated wet granulation processes: a review. *Powder Technol.* 2001;117(1–2): 3–39.
2. Knight PC, Instone T, Pearson JMK, Hounslow MJ. An investigation into the kinetics of liquid distribution and growth in high shear mixer agglomeration. *Powder Technol.* 1998;97:246–257.
3. Schæfer T, Mathiesen C. Melt pelletization in a high shear mixer IX. Effects of binder particle size. *Int. J. Pharmaceut.* 1996;139:139–148.
4. Schæfer T, Mathiesen C. Melt pelletization in a high shear mixer VIII. Effects of binder viscosity. *Int. J. Pharmaceut.* 1996;139:125–128.
5. Scott AC, Hounslow MJ, Instone T. Direct evidence of heterogeneity during high-shear granulation. *Powder Technol.* 1999;113:215–213.
6. Chouk V, Reynolds G, Hounslow M, Salman A. Single drop behaviour in a high shear granulator. *Powder Technol.* 2009;189(2):357–364.
7. Schaafsma SH, Vonk P, Kossen NWF, Hoffmann AC. A model for the spray zone in early-stage fluidized bed granulation. *AIChE J.* 2006;52(8):2736–2741.
8. Hapgood KP, Litster JD, Biggs SR, Howes T. Drop penetration into porous powder beds. *J. Colloid Interface Sci.* 2002; 253(2):353–366.
9. Litster JD, Hapgood KP, Michaels JN, Sims A, Roberts M, Kameneni SK, Hsu T. Liquid distribution in wet granulation: dimensionless spray flux. *Powder Technol.* 2001; 114(1–3):32–39.
10. Hapgood KP, Litster JD, Smith R. Nucleation regime map for liquid bound granules. *AIChE J.* 2003;49(2):350–361.
11. Litster JD, Hapgood KP, Michaels JN, Sims A, Roberts M, Kameneni SK. Scale-up of mixer granulators for effective liquid distribution. *Powder Technol.* 2002; 124(3):272–280.
12. Hapgood KP, Litster JD, White ET, Mort PR, Jones DG. Dimensionless spray flux in wet granulation: Monte-Carlo simulations and experimental validation. *Powder Technol.* 2004;141(1–2):20–30.
13. Wildeboer WJ, Litster JD, Cameron IT. Modelling nucleation in wet granulation. *Chem. Eng. Sci.* 2005;60:3751–3761.
14. Hapgood KP, Nguyen TH, Hauw S, Iveson SM, Shen W. Rewetting effects and droplet motion on partially wetted powder surfaces. *AIChE J.* 2009;55(6):1402–1415.
15. Denesuk M, Smith GL, Zelinski BJJ, Kreidl NJ, Uhlmann DR. Capillary penetration of liquid droplets into porous materials. *J. Colloid Interface Sci.* 1993;158:114–120.
16. Middleman S. *Modelling Axisymmetric Flows: Dynamics of Films, Jets, and Drops*, Chapter 8, Academic Press, San Diego, 1995, p. 299.
17. Ax K, Feise H, Sochon R, Hounslow M, Salman A. Influence of liquid binder dispersion on agglomeration in an intensive mixer. *Powder Technol.* 2008;179(3):190–194.

18. Hapgood KP. *Nucleation and Binder Dispersion in Wet Granulation*, PhD thesis, Department of Chemical Engineering, University of Queensland, Brisbane, Australia, 2000.
19. Schaafsma SH, Vonk P, Segers P, Kossen NWF. Description of agglomerate growth. *Powder Technol.* 1998;97:183–190.
20. Waldie B. Growth mechanism and the dependence of granule size on drop size in fluidised bed granulation. *Chem. Eng. Sci.* 1991;46(11):2781–2785.
21. Plank R, Diehl B, Grinstead H, Zega J. Quantifying liquid coverage and powder flux in high-shear granulators. *Powder Technol.* 2003;134(3):223–234.
22. Hapgood KP, Amelia R, Zaman MB, Merrett BK, Leslie P. Improving Liquid Distribution by Reducing Dimensionless Spray Flux in Wet Granulation—A Pharmaceutical Manufacturing Case Study. In: *9th International Symposium on Agglomeration*, Sheffield University, Sheffield, UK, 2009.
23. Wildeboer WJ, Koppendraaier E, Litster JD, Howes T, Meesters G. A novel nucleation apparatus for regime separated granulation. *Powder Technol.* 2007;171(2):96–105.
24. Wauters PAL, Jakobsen RB, Litster JD, Meesters GMH, Scarlett B. Liquid distribution as a means to describing the granule growth mechanism. *Powder Technol.* 2002;123:166–177.
25. Schaafsma SH, Kossen NWF, Mos MT, Blauw L, Hoffman AC. Effects and control of humidity and particle mixing in fluid-bed granulation. *AIChE J.* 1999;45(6):1202–1210.
26. Vonk P, Guillaume CPF, Ramaker JS, Vromans H, Kossen NWF. Growth mechanisms of high-shear pelletisation. *Int. J. Pharmaceut.* 1997;157:93–102.
27. Hapgood KP, Tan MXL, Chow DWY. Predicting nuclei size distributions in wet granulation using dimensionless spray flux. *Adv. Powder Technol.* 2009; 20(4): p. 293–297.
28. Marshall WRJ. Atomization and spray drying. *Chem. Eng. Progress,* Monograph Series 1954;50(2).
29. Stewart RL, Bridgwater J, Parker DJ. Granular flow over a flat-bladed stirrer. *Chem. Eng. Sci.* 2001;56:4257–4271.
30. Laurent BFC. Scaling factors in granular flow: analysis of experimental and simulations results. *Chem. Eng. Sci.* 2006;61(13):4138–4146.
31. Forrest S, Bridgwater J, Mort PR, Litster J, Parker DJ. Flow patterns in granulating systems. *Powder Technol.* 2003;130:91–96.
32. Laurent BFC, Bridgwater J, Parker DJ. Motion in a particle bed agitated by a single blade. *AIChE J.* 2000; 46(9):1723–1734.
33. Tardos GI, Hapgood KP, Ipadeola OO, Michaels JN. Stress measurements in high-shear granulators using calibrated test particles: application to scale-up. *Powder Technol.* 2004; 140(3):217–227.
34. Hapgood K, Jain S, Kline L, Moaddeb M, Zega J. Application of Spray Flux in Scale-Up of High Shear Wet Granulation Processes. In: *AIChE Annual Meeting*, AIChE, San Francisco, 2003.
35. Iveson SM, Beathe JA, Page NW. The dynamic strength of partially saturated powder compacts: the effect of liquid properties. *Powder Technol.* 2002;127:149–161.
36. Iveson SM, Page N. *Dynamic mechanical properties of liquid bound powder compacts*, *in 3rd Australasian Congress on Applied Mechanics (ACAM2002)*, Sydney, Australia: World Scientific, 2002.
37. Iveson SM, Page N. Brittle to plastic transition in the dynamic mechanical behavior of partially saturated granular materials. *Trans. ASME* 2004;71:470–475.
38. Iveson SM, Page N. Dynamic strength of liquid-bound granular materials: the effect of particle size and shape. *Powder Technol.* 2005;152:79–89.
39. Iveson SM, Litster JD, Ennis BJ. Fundamental studies of granule consolidation. Part 1: effects of binder content and binder viscosity. *Powder Technol.* 1996;88:15–20.
40. Iveson SM, Litster JD. Fundamental studies of granule consolidation. Part 2: quantifying the effects of particle and binder properties. *Powder Technol.* 1998;99:243–250.
41. Zoglio MA, Cartensen JT. Physical aspects of wet granulation III. Effect of wet granulation on granule porosity. *Drug Dev. Ind. Pharm.* 1983;9(8):1417–1434.
42. Ohno I, Hasegawa S, Yada S, Kusai A, Moribe K, Yamamoto K. Importance of evaluating the consolidation of granules manufactured by high shear mixer. *Int. J. Pharmaceut.* 2007;338(1–2):79–86.
43. Farber L, Tardos G, Michaels JN. Use of X-ray tomography to study the porosity and morphology of granules. *Powder Technol.* 2003;132(1):57–63.
44. Ansari MA, Stepanek F. Formation of hollow core granules by fluid bed *in situ* melt granulation: modelling and experiments. *Int. J. Pharmaceut.* 2006;321(1–2):108–116.
45. Ansari MA, Stepanek F. Design of granule structure: computational methods and experimental realization. *AIChE J.* 2006;52(11):3762–3774.
46. Hapgood KP, Farber L, Michaels JN. Agglomeration of hydrophobic powders via solid spreading nucleation. *Powder Technol.* 2009;188(3):248–254.
47. Rahmanian N, Ghadiri M, Jia X, Stepanek F. Characterisation of granule structure and strength made in a high shear granulator. *Powder Technol.* 2009;192(2):184–194.
48. Jægerskou A, Holm P, Schæfer T. Granulation in high speed mixers. Part 3: effects of process variables on the intragranular porosity. *Pharm. Ind.* 1984;46(3):310–314.
49. Berggren J, Alderborn G. Effect of drying rate on porosity and tabletting behaviour of cellulose pellets. *Int. J. Pharmaceut.* 2001;227:81–96.
50. Mort PR. Scale-up of binder agglomeration processes. *Powder Technol.*150(2): 2005; 86–103.
51. Iveson SM. *Fundamental Studies of Granulation: Granule Deformation and Consolidation*, University of Queensland, Brisbane, Australia, 1997.
52. Iveson SM, Litster JD. Growth regime map for liquid-bound granules. *AIChE J.* 1998;44(7):1510–1518.
53. Wauters PAL, van de Water R, Litster JD, Meesters GMH, Scarlett B. Growth and compaction behaviour of copper concentrate granules in a rotating drum. *Powder Technol.* 2002;124(3):230–237.

54. Iveson SM, Wauters PAL, Forrest S, Litster JD, Meesters GMH, Scarlett B. Growth regime map for liquid-bound granules: further development and experimental validation. *Powder Technol.* 2001;117:83–97.
55. Tu W-D, Hsiau S-S, Ingram A, Seville J. The effect of powder size on induction behaviour and binder distribution during high shear melt agglomeration of calcium carbonate. *Powder Technol.* 2008;184(3):298–312.
56. Hoornaert F, Wauters PAL, Meesters GMH, Pratsinis SE. Agglomeration behaviour of powders in a Lödige mixer granulator. *Powder Technol.* 1998;96:116–128.
57. Mackaplow MB, Rosen LA, Michaels JN. Effect of primary particle size on granule growth and endpoint determination in high-shear wet granulation. *Powder Technol.* 2000; 108(1):32–45.
58. Litster JD, Ennis BJ. *The Science and Engineering and Granulation Processes*, Kluwer Academic Publishers, Dordrecht, 2004.
59. Ennis BJ, Li J, Tardos GI, Pfeffer R. The influence of viscosity on the strength of an axially strained pendular liquid bridge. *Chem. Eng. Sci.* 1990;45(10):3071–3088.
60. He Y, Liu LX, Litster JD, Kayrak-Talay D. Scale up considerations in granulation. In: Parikh DM, editor, *Handbook of Pharmaceutical Granulation*, Taylor and Francis Group, Boca Raton, FL, 2009, pp. 459–490.
61. Ennis BJ, Litster JD. Size reduction and size enlargement., In: Green D, editor, *Perry's Chemical Engineers' Handbook*, McGraw-Hill, New York, 1997.
62. Reynolds GK, Fu JS, Cheong YS, Hounslow MJ, Salman AD. Breakage in granulation: a review. *Chem. Eng. Sci.* 2005; 60(14):3969–3992.
63. Fu JS, Reynolds GK, Adams MJ, Hounslow MJ, Salman AD. An experimental study of the impact breakage of wet granules. *Chem. Eng. Sci.* 2005;60(14):4005–4018.
64. Tardos GI, Khan MI, Mort PR. Critical parameters and limiting conditions in binder granulation of fine powders. *Powder Technol.* 1997;94:245–258.
65. Smith R. *Wet Granule Breakage in High Shear Mixer Granulators*, PhD Thesis, Department of Chemical Engineering, University of Queensland, Brisbane, Australia, 2008.
66. Smith RM, Litster JD, Page NW. Diametrical compression of wet granular materials. *Powder Technol.* 2010; Submitted.
67. Iveson SM, Page NW, Litster JD. The importance of wet-powder dynamic mechanical properties in understanding granulation. *Powder Technol.* 2003;130:97–101.
68. van den Dries K, Vegt OMd, Girard V, Vromans H. Granule breakage phenomena in a high shear mixer; influence of process and formulation variables and consequences on granule homogeneity. *Powder Technol.* 2003;113:228–236.
69. Smith RM, Liu LX, Litster JD. Breakage of drop nucleated granules in a breakage only high shear mixer. *Chem. Eng. Sci.* 2010; doi:10.1016/j.ces.2010.06.037.
70. Liu LX, Smith R, Litster JD. Wet granule breakage in a breakage only high-hear mixer: effect of formulation properties on breakage behaviour. *Powder Technol.* 2009; 189(2):158–164.
71. Knight PC, Johansen A, Kristensen HG, Schæfer T, Seville JPK. An investigation of the effects on agglomeration of changing the speed of a mechanical mixer. *Powder Technol.* 2000;110:204–209.
72. Pearson JKM, Hounslow MJ, Instone T. Tracer studies of high-shear granulation I: experimental results. *AIChE J.* 2001;47(9):1978–1983.
73. Ramaker JS, Jelgersma MA, Vonk P, Kossen NWF. Scale-down of a high shear pelletisation process: flow profile and growth kinetics. *Int. J. Pharmaceut.* 1998;166:89–97.
74. Hounslow MJ, Pearson JMK, Instone T. Tracer studies of high-shear granulation: II population balance modeling. *AIChE J.* 2001;47(9):1984–1999.
75. Bouwman AM, Visser MR, Meesters GMH, Frijlink HW. The use of Stokes deformation number as a predictive tool for material exchange behaviour of granules in the 'equilibrium phase' in high shear granulation. *Int. J. Pharmaceut.* 2006; 318(1–2):78–85.
76. Tran A. Powder flow in mixer granulators. In: *Chemical Engineering*, University of Queensland, Brisbane, Australia, 2010.
77. Holm P, Jungersen O, Schæfer T, Kristensen HG. Granulation in high speed mixers. Part 1 effects of process variables during kneading. *Pharm. Ind.* 1983;45(8):806–811.
78. Holm P, Jungersen O, Schæfer T, Kristensen HG. Granulation in high speed mixers. Part 2 effects of process variables during kneading. *Pharm. Ind.* 1984;46(1):97–101.
79. Holm P. Effect of impeller and chopper design on granulation in a high speed mixer. *Drug Dev. Ind. Pharm.* 1987; 13(9–11):1675–1701.
80. Johansen A, Schæfer T. Effects of interactions between powder particle size and binder viscosity on agglomerate growth mechanisms in a high shear mixer. *Eur. J. Pharmaceut. Sci.* 2001;12:297–309.
81. Michaels JN, Farber L, Wong GS, Hapgood K, Heidel SJ, Farabaugh J, Chou JH, Tardos GI. Steady states in granulation of pharmaceutical powders with application to scale-up. *Powder Technol.* 2009;189(2):295–303.
82. Aulton M, Banks M. The factors affecting fluidised bed granulation. *Manuf. Chemist Aer. N.* 1978;49:50–56.
83. Capes CE. *Particle Size Enlargement*, Elsevier Scientific Publishing Company, Amsterdam, 1980.
84. Rambali B, Baert L, Massart DL. Scaling up of the fluidized bed granulation process. *Int. J. Pharmaceut.* 2003;252:197–206.
85. Hapgood K, Plank R, Zega J. Use of Dimensionless Spray Flux to Scale Up a Wet Granulated Product. In: *World Congress on Particle Technology 4*, Sydney, Australia, 2002.
86. Stewart RL, Bridgwater J, Zhou YC, Yu AB. Simulated and measured flow of granules in a bladed mixer—a detailed comparison. *Chem. Eng. Sci.* 2001;56:5457–5471.
87. Laurent BFC, Bridgwater J. Performance of single and six-bladed powder mixers. *Chem. Eng. Sci.* 2002;57: 1695–1709.

88. Nilpawar AM, Reynolds GK, Salman AD, Hounslow MJ. Surface velocity measurement in a high shear mixer. *Chem. Eng. Sci.* 2006;61(13):4172–4178.
89. Reynolds GK, Nilpawar AM, Salman AD, Hounslow MJ. Direct measurement of surface granular temperature in a high shear granulator. *Powder Technol*. 2008;182(2):211–217.
90. Hiseman MJP, Bridgwater J, Wilson DI. Positron Emission Particle Tracking Studies of Powder Mixing in a Planetary Mixer. In: *Control of Particulate Processes IV*, Engineering Foundation, Delft, Netherlands, 1997.
91. Horsthuis GJB, Laarhoven JAHV, van Rooij RCMB, Vromans H. Studies on upscaling parameters of the Gral high shear granulation process. *Int. J. Pharmaceut*. 1993;92:143–150.
92. Litster JD, Hapgood KP, Michaels JN, Kamineni SK, Sims A, Roberts M, Hsu T. Scale-Up of Mixer Granulators for Effective Liquid Distribution. In: *Control of Particulate Processes 6*, Engineering Foundation, Fraser Island, Australia, 1999.
93. Rahmanian N, Ghadiri M, Ding Y. Effect of scale of operation on granule strength in high shear granulators. *Chem. Eng. Sci.* 2008;63(4):915–923.
94. Knight PC, Seville JPK, Wellm AB, Instone T. Prediction of impeller torque in high shear powder mixers. *Chem. Eng. Sci.* 2001;56:4457–4471.
95. Landin M, York P, Cliff MJ, Rowe RC, Wigmore AJ. Scale-up of pharmaceutical granulation in fixed bowl mixer-granulation. *Int. J. Pharmaceut.* 1996;133:127–131.
96. Hassanpour A, Antony SJ, Ghadiri M. Modeling of agglomerate behavior under shear deformation: effect of velocity field of a high shear mixer granulator on the structure of agglomerates. *Adv. Powder Technol.* 2007;18:803–811.
97. Fu J, Chan EL, Jones MR, Kemp IC, Gilmour CM, Hounslow MJ, Salman AD. Characterisation of impact stress from main impeller on granules during granulation processes in a high shear mixer. In: Salman AD, editor, *9th International Symposium on Agglomeration*, Sheffield University, Sheffield, UK, 2009.
98. Mort PR. Scale-up and control of binder agglomeration processes—flow and stress fields. *Powder Technol*. 2009;189(2):313–317.
99. Faure A, Grimsey IM, Rowe RC, York P, Cliff MJ. Applicability of a scale-up method for wet granulation processes in Collette Gral high shear mixer-granulators. *Eur. J. Pharmaceut. Sci.* 1999;8:85–93.
100. Stepanek F, Rajniak P, Mancinelli C, Chern R, Determination of the Coalescence Probability of Wet Granules by Mesoscale Modeling. In: *AIChE Annual Meeting*, AIChE, San Francisco, CA, 2006.
101. Boerefijn R, Juvin PY, Garzon P. A narrow size distribution on a high shear mixer by applying a flux number approach. *Powder Technol*. 2009;189(2):172–176.
102. Hapgood KP, Khanmohammadi B. Granulation of hydrophobic powders. *Powder Technol*. 2009;189(2):253–262.
103. Vervaet C, Remon JP. Continuous granulation in the pharmaceutical industry. *Chem. Eng. Sci.* 2005;60(14):3949–3957.
104. Djuric D, Kleinebudde P. Impact of screw elements on continuous granulation with a twin-screw extruder. *J. Pharmaceut. Sci.* 2009;97(11):4934–4942.
105. Hu X, Cunningham JC, Winstead D. Study growth kinetics in fluidized bed granulation with at-line FBRM. *Int. J. Pharmaceut.* 2008;347(1–2):54–61.
106. Cantor SL, Kothari S, Koo OMY. Evaluation of the physical and mechanical properties of high drug load formulations: wet granulation vs. novel foam granulation. *Powder Technol*. 2009;195(1):15–24.
107. Keary CM, Sheskey PJ. Preliminary report of the discovery of a new pharmaceutical granulation process using foamed aqueous binders. *Drug Dev. Ind. Pharm.* 2004;30(8):831–845.
108. Tan MXL, Wong LS, Lum KH, Hapgood KP. Foam and drop penetration kinetics into loosely packed powder beds. *Chem. Eng. Sci.* 2009;64(12):2826–2836.